Order Number 1352397

Modelling of end milling operation to predict the achievable surface finish and tolerance

Kulkarni, Nitin Madhukar, M.S.

The University of Arizona, 1993

U·M·I
300 N. Zeeb Rd.
Ann Arbor, MI 48106

MODELLING OF END MILLING OPERATION TO PREDICT THE ACHIEVABLE SURFACE FINISH AND TOLERANCE

by

Nitin Madhukar Kulkarni

A Thesis Submitted to the Faculty of the

DEPARTMENT OF AEROSPACE AND MECHANICAL ENGINEERING

In Partial Fulfillment of the Requirements
For the Degree of

MASTER OF SCIENCE
WITH A MAJOR IN MECHANICAL ENGINEERING

In the Graduate College

THE UNIVERSITY OF ARIZONA

1 9 9 3

STATEMENT BY THE AUTHOR

This thesis has been submitted in partial fulfillment of requirements for an advanced degree at The University of Arizona and is deposited in the University Library to be made available to borrowers under rules of the Library.

Brief quotations from this thesis are allowable without special permission, provided that accurate acknowledgment of source is made. Requests for permission for extended quotation from or reproduction of this manuscript in whole or in part may be granted by the head of the major department or the Dean of the Graduate College when in his or her judgment the proposed use of the material is in the interests of scholarship. In all other instances, however, permission must be obtained from the author.

SIGNED: 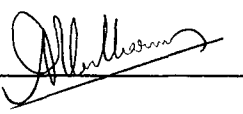

APPROVAL BY THESIS DIRECTOR

This thesis has been approved on the date shown below:

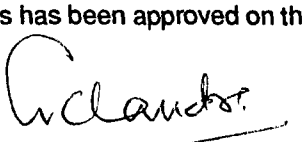

Dr. A. Chandra,
Associate Professor
Dept. of Aerospace and Mechanical Engineering

Jan 8, 1993

Date

ACKNOWLEDGEMENTS

I would like to thank my advisor, Professor Abhijit Chandra, for giving me the opportunity to carry out this research project. His advise, suggestions, and insights were invaluable to both this project and my education.

I would also like to thank Professor Sanjay Jagdale (Systems and Industrial Engineering), for his valuable guidance and suggestions for this research, specially during the early formative stages of this project.

Finally I would like to thank my colleagues and friends, CCIT and workshop personnel, without whose cooperation this project would not have been possible.

TABLE OF CONTENTS

TABLE OF CONTENTS - *Continued*

LIST OF ILLUSTRATIONS

LIST OF ILLUSTRATIONS - *Continued*

LIST OF TABLES

ABSTRACT

With increasing necessity to integrate CAD and CAM, it is necessary to develop more accurate models for predicting the performance of manufacturing processes. Conventionally, process parameters are selected by the process planner based on his experience. For CAD-CAM integration to be meaningful, it should be possible to arrive at the same decisions using computer models for that process. The end milling process is selected for such modeling. The parameters considered are process variables, cutter geometry, cutter material properties, workpiece material properties, workpiece geometry and location and properties of inclusions (if any) in the material. Dynamic Model for end milling is developed and successive iterations are performed to arrive at the speed and feed required to generate a given surface finish and tolerance.

CHAPTER 1

INTRODUCTION

Various milling models are found in the literature. These tend to be narrow and application specific. The approach of these models is to predict the surface finish and tolerance achieved, given a certain set conditions. These may be in the form of process variables, cutter variables and/or machine tool constants. We therefore have a number of different models, which have been reviewed in the literature survey. However, the problem faced by production shops is the other way round. A manufacturing engineer is called upon by the design engineer to manufacture a given part with a required tolerance and surface finish. The manufacturing engineer then makes a process plan to meet his requirements, depending upon the resources available to him. This consists of the machines available in his production shop and cutting tools from his tool inventory. The variables available for manipulation, therefore, are the speed, feed, and cutting tool variables.

A general purpose model with variables normally available for manipulation should therefore be set up. It should also be possible to extend the model further to include parameters which are peculiar to a given situation and which impose constraints due to the fact that they cannot be manipulated.

Typically, process variables (for example, speed, feed, depth of cut (radial and axial)) and cutter geometry (for example, helix angle, rake angle, cutter overhang) are within the control of any production shop. On the other hand, machine tool parameters (for example, machine dynamics, spindle run-out and accuracy) are not, since their variation is limited to the machines available in the shop. These variables are therefore a constraint. It is therefore proposed to build a model, that incorporates these normally variable parameters, to predict the optimum achievable

surface finish and tolerance. The model should then allow incorporating the machine tool parameters for a particular machine to predict the surface finish and tolerance achievable on that machine.

Such a model will also assist in the integration of CAD and CAM. For a given tolerance and surface finish required for the manufacture of a part, the possibility of manufacture by milling can not only be determined, but also the optimum process parameters calculated and incorporated in the CAM program. As every production shop has a variety of machines which differ in make, model and accuracy, the milling model will be able to predict which machines are capable of doing the job once the machine parameters are known. Scheduling of the job will then be facilitated.

For a milling process for instance, the manufacturing engineer has to decide on the following:

1. Selection of the cutter
2. Selection of feed and speed
3. Selection of the correct milling machine

In selecting the cutter, selection has to be made regarding the cutter material, diameter, number of teeth, helix angle and cutter length. Design synthesis in chapter 9 gives details of rules and guidelines on selection of these. The Dynamic model is used in analyzing the effect of each of these. Selection of feed and speed is based on experience of the manufacturing engineer and it is this aspect of the selection that is investigated here. Selection of the machine tool is no selection at all, as the engineer is restricted to the machines available in his shop. This is therefore a constraint and not a choice.

The proposed model therefore takes care of the above conditions. It allows input of cutter variables and predicts the speed and feed to achieve the required surface finish. This is the general purpose model for the milling process itself. The model makes provision for its

modification to incorporate the machine tool specific parameters so that prediction of speed and feed for a specific situation (i.e. for a specific production shop) is possible.

The following variables have to be input to the model:

1. Process Variables :
   - 1.1 Maximum allowable speed for a given combination of cutting tool and work-piece material.
   - 1.2 Maximum allowable feed for a given combination of cutting tool and work-piece material.
   - 1.3 Radial depth of cut.
   - 1.4 Axial depth of cut.
   - 1.5 Desired surface finish
2. Cutter Variables
   - 2.1 Cutter diameter
   - 2.2 Number of teeth
   - 2.3 Helix angle
   - 2.4 Cutter length
   - 2.5 Cutter elastic constant
   - 2.6 Cutter material density
   - 2.7 Cutter damping ratio
3. Computational Variables
   - 3.1 Number of levels into which the axial depth of cut is to be divided.
   - 3.2 Number of time intervals into which one revolution of the cutter is to be divided.
   - 3.3 Number of revolutions to model.
   - 3.4 Number of points to be considered in one feed per tooth, for computing the surface finish.
   - 3.5 Dynamic coefficient for the dynamic model.

3.6 Error level for iteration.

4. Geometric features of workpiece

4.1 Coordinates of the four points that represent the geometric feature.

5. Inclusion variables

5.1 Inclusion material properties.

5.2 Inclusion locations.

The model then iterates with various feed and speeds and comes up with recommended values to achieve the given surface finish. The model is general purpose, at present. But it can be modified to include the machine tool variables to tailor it for a particular situation.

The model thus built becomes a tool to analyze the effect of various parameters on the surface finish. The chapter on design synthesis gives the analysis and conclusions based on the investigations into parameter variations. The model was run on Convex, a parallel processor machine, for various sets of parameters. Comparison with experimental results of other investigators have been found to match very well.

CHAPTER 2

LITERATURE SURVEY

Several models for the milling process are found in the literature. From [1] they can be classified into the following:

1) Average Rigid Force Static Deflection Model

2) Instantaneous Rigid Force Model.

3) Instantaneous Rigid Force, Static Deflection Model.

4) Instantaneous Rigid Force with Static Deflection Feedback Model.

5) Regenerative Force, Dynamic Deflection Model.

2.1 Average Rigid Force Static Deflection Model

This is the simplest of all models and is useful as a first approximation to compute the forces and cutter deflection in milling. The model relies on the relationship between metal removal rate and the average power consumed in the cut.

$$P = P_{sp}\, d_a\, d_r\, T\, f_t\, n \qquad (2.1)$$

where

P = Power

P_{sp} = Specific Power

d_a = Axial depth of cut

d_r = Radial depth of cut

T = number of teeth

f_t = feed per tooth

n = rpm of the cutter

The average cutting force is then

$$F_t = \frac{P}{v}$$

where

v = peripheral velocity

The force acting to deflect the cutter is now taken to be half of the computed cutting force.

$$F_n = 0.5\, F_t$$

Deflection of the cutter is then computed by considering the side thrust force as a concentrated load acting at the end of the cutter modeled as a cantilever beam. The error in location of the surface is taken as equal to this deflection.

Such a model was used by Wang [2] in solid modeling for optimizing metal removal of three dimensional end milling.

2.2 Instantaneous Rigid Force Model

This is a refinement of the above model specifically with respect to the computation of the milling forces. Even without considering the effect of the deflection of the cutter on the force, it is clear that the cutting force is not constant, because the chip thickness varies with cutter rotation. The chip thickness also varies with the axial depth of the cut in the case of a helical cutter. This fact is incorporated in the this model which establishes cutting force as a function of the chip thickness. The cutter is assumed rigid for computing the chip thickness which is given from [14] as

$$b = f_t \sin \phi$$

f_t = feed per tooth

ϕ = angle of rotation of the cutter

The cutter is divided into a number of slices as shown in fig 2.1 and on each slice, the incremental force in up milling is given as

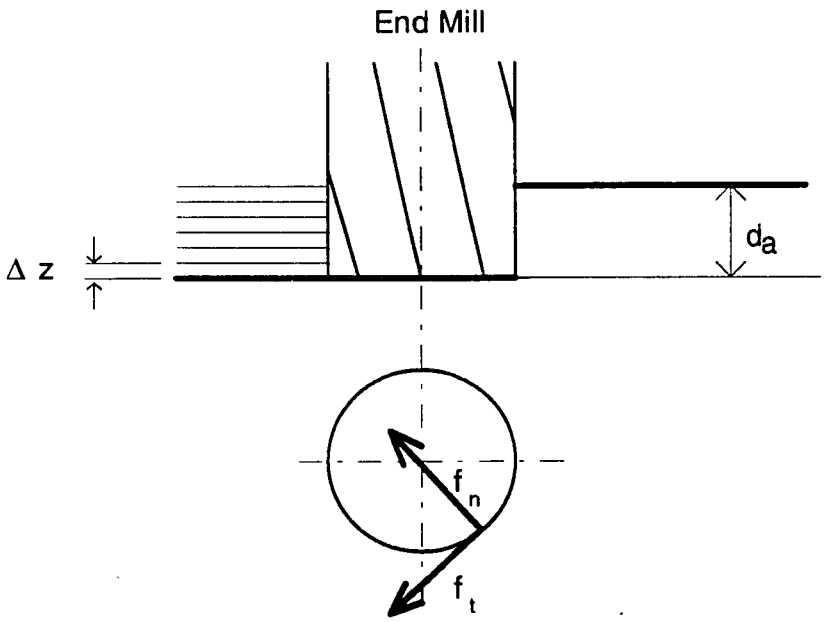

Fig 2.1 Forces on each slice of the end mill

$$f_{ti} = K_{st}\, b\, \Delta z$$

$$f_{ni} = K_{sn}\, b\, \Delta z$$

where

f_{ni} = incremental force on slice i, in the normal direction

f_{ti} = incremental force on slice i, in the tangential direction

K_{sn} = force constant of proportionality in the normal direction

K_{st} = force constant of proportionality in the tangential direction

b = chip thickness for slice i, at the given instant

Δz = thickness of the slice

The total instantaneous force is then the summation over the axial depth for all teeth cutting at that given instant. This model is was used by Tlusty [4] and DeVor [3] for predicting milling forces.

2.3 Instantaneous Rigid Force, Static Deflection Model

This model is an extension of the above model, in that it also predicts the cutter deflection and surface finish generated.

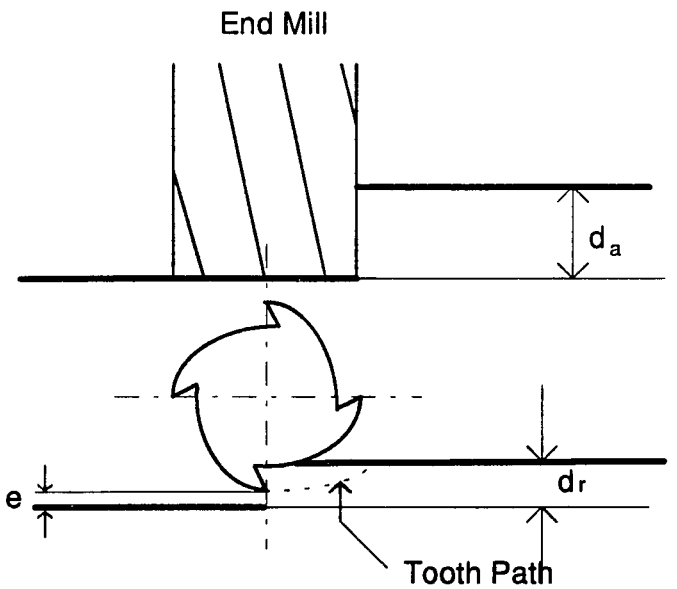

Fig 2.2 Deflected tooth path

As shown in fig 2.2, d_r is the radial depth of cut and d_a is the axial depth of cut. The deflection of the cutter results in a surface that is a distance e away from the required surface. Having calculated the cutter deflections at all points, it is possible to compute the surface generated. This model is used as a basis here for computing static deflections, and is discussed in detail in the chapter on Deflection model. Tlusty [5], Hann [6] and Kline et al [7] have used this model for computing cutter deflections and profile of the surface generated.

2.4 Instantaneous Rigid Force with Static Deflection Feedback Model

This model takes into account the change in the cutting force due to the deflection of the cutter. As the cutter deflects, the chip thickness changes, thus changing the cutting force. The change in cutting force changes the deflection, thus changing chip thickness again. This relationship is shown in [8] to be a geometric progression. The final position of the cutter is computed using a geometric series. Since the effect of the instantaneous force on the cutter is taken into account, it is called the instantaneous force with static deflection feed back model. The cutter deflection is now given by

$$\delta = \frac{\frac{k_s b}{k}}{1+\frac{k_s b}{k}} c \qquad (2.4)$$

where

k = cutter stiffness

k_S = force constant

2.5 Regenerative Force, Dynamic Deflection Model

The last model is of sufficient complexity and apart from the above, also takes into account the machine dynamics as well as the fact that the cutting force depends not only on the feed per tooth, and on the deflection of the cutter as before, but also on the surface which was left by the passage of the previous tooth. This model is used here and is discussed in detail in the chapter on Dynamic model. This model was used by Tlusty et al. [17] in their study of chatter in milling.

In all the above models, computation of the cutting force plays an important part in the accuracy of the results. Excluding the first model, which uses specific power of metal removal, all models incorporate some sort of experimentally determined constant to calculate the cutting

force. Watanabe [12] calculated the cutting force from shear stress and shear angle in which the shear stress was measured from the bending moments. Stephenson [13] argued that the conditions during metal cutting are so severe that they cannot be equated to any normal properties of the metal. The cutting forces, shear stress and friction coefficient during metal cutting can only be related to the same parameters obtained from standard metal cutting test. Here, cutting forces are computed using the single point orthogonal cutting model for each tooth of the milling cutter, at each slice. The force constants are computed on equations taken from [15], where angle of the shear plane is related to the ultimate and yield strength of the material.

However, all models above predict the surface finish given several input parameters, among them speed and feed. An attempt is made here to predict the speed and feed, given the required surface finish. This is a new approach to the whole problem.

CHAPTER 3

OVERVIEW OF THE ITERATING APPROACH

The basis for all models is the rigid cutter-rigid machine model. This model was first proposed by Martellotti [14]. It refers to the most ideal condition, and an insight into the milling process itself is obtained by studying this model.

Martellotti derived the following expression for the surface finish obtained in the milling process and is given as under:

$$h = \frac{f_t^2}{8\left[R + \frac{f_t T}{\pi}\right]} \qquad (3.1)$$

f_t = Feed per tooth

R = Cutter radius

h = height of uncut material

T = Number of teeth of the cutter

Conventional milling machines during the time of Martellotti (1941) derived their table feed from the spindle by a gear train, and therefore it was always a fixed ratio. Hence the concept of feed per tooth was common. However modern CNC milling machines no longer have their speed and feed related to each, as each can be independently programmed. It is therefore necessary to update the above equation to incorporate this change. Choosing Feed and Speed as independent variables, the equation changes to

$$h = \frac{\pi F^2}{8\pi T^2 n^2 R + 8T^2 F n} \tag{3.2}$$

F = Feed (distance/time)

T = Number of teeth of the cutter

n = rpm of the spindle

R = Radius of the cutter

The same equation is applicable for up-milling and down-milling. However, in the case of up-milling, if both F and n are taken to be positive, in down milling either one has to be taken as is negative.

In order to optimize the speed and feed required to obtain the best surface finish, it is necessary to examine how the surface finish varies in this ideal condition. The expression for h therefore has to be partially differentiated with respect to speed and feed, to obtain the best combination. Considering the case of up-milling, when both F and n are positive, the partial differentiation with respect to both F and n gives the following result:

$$\frac{\partial h}{\partial n} = 2\pi R n + F \tag{3.3}$$

$$\frac{\partial h}{\partial F} = 2\pi R n + F \tag{3.4}$$

This has only the trivial solution, i.e., F = 0 and n = 0

A greater analysis of the function is necessary. A plot of this function is shown in fig.3.11 on page 26

It can be seen that as rpm increases, with constant feed, the height of uncut surface decreases. Also as feed increases, for a constant rpm, the height of uncut surface increases. As

the function has a trivial minimum, it can be inferred that it is theoretically possible to obtain any required surface finish. However, this is not practical. There are constraints on the maximum speed as well as the feed. The limitations on the speed may be due to the following

(1) Maximum cutting velocity permissible for a given combination of work-piece material and cutting tool.

(2) Maximum cutting velocity (distance/time) permissible to obtain a given tool life.

(3) Maximum speed (revolutions/time) available on a given machine.

(4) Maximum speed permissible to avoid chatter on a given machine.

The limitations on the feed can be due to the machine tool itself.

It is for the user to identify the limits on the velocity arising due to problem at hand. As this thesis is limited to building a general purpose model alone, the machine tool constraints are not included. But a provision is made to include and extend the model in the future.

The feasible region is then as shown in fig 3.12 on page 26, where the shaded area covers the region with rpm less than the permissible speed and feed less than the permissible feed.

Once the maximum permissible velocity is identified, the corresponding speed for the chosen cutter is calculated. The rigid cutter model is first used to calculate the feed for the required surface finish as under:

$$F = A \pm C$$

where

$$A = \frac{4T^2nh}{p}$$

$$C = \frac{2T^2n}{p}D$$

$$D = \sqrt{(4T^2h^2+2p^2Rh)}$$

Since $\frac{C}{A} = \frac{D}{2h}$, which is always >1, C >A. As negative F is not acceptable, we only take the positive F. Therefore,

$$F = A + C$$

When the speed is a constraint, the calculated feed for a given surface finish is as shown in fig 3.13. on page 26.

However, if the calculated feed is above the permissible feed for the process, the rigid cutter model is used again, but this time the limiting feed is taken and the corresponding speed is calculated as under.

The quadratic equation for n derived from (3.2) is as under

$$8\pi T^2 n^2 Rh + 8T^2 Fnh - \pi F^2 = 0 \qquad (3.5)$$

from which n is calculated.

The feed now is the constraint, and the resultant rpm is computed as above is shown in fig 3.14 on page 26.

Both the above constraints, have given us a limiting rpm: $N_{max.}$ This would be the starting point of the iterations for the speed and feed, as the various models are successively implemented.

Deflection Model is considered next. It can be inferred that as cutter deflection is considered, the surface finish will get worse and consequently the uncut height h will increase. Either n will have to be increased or F decreased to maintain the same h. Since n is already at the maximum possible level, (due to either velocity limitations or feed limitations) F will have to be reduced. However, there is no closed expression for obtaining h in the Deflection Model. For a given n and F, h is obtained by numerical integration. It is therefore necessary to have an iterating process, by which F and n for a given h can be found. Fig 3.2 illustrated how successive iterations can be performed to calculate values of F and n.

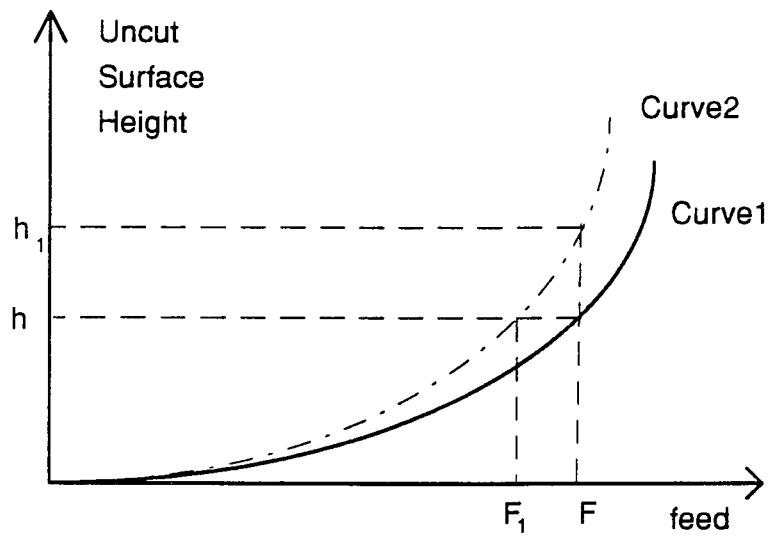

Fig 3.2 Iteration method

It is reasonable to assume that h, F and n behave in the same way in the deflection and dynamic models as in the rigid cutter model. Therefore the relation between h and F for a constant n can be approximated as under:

$$h = \frac{F^2}{C+F} \tag{3.6}$$

where C is a constant. We begin with the values of F and n obtained from the rigid cutter model. These are used in the deflection model to predict the uncut height, say h_1. If curve1 represents the Rigid cutter model, then curve2 can be assumed to represent the dynamic/deflection model for the same rpm. F and h_1 are therefore points on this curve which has a constant C given by

$$C = \frac{F^2}{h_1} - F \tag{3.7}$$

This value of C is then used in (3.6) to predict the value of feed for the desired h. This can be seen as F_1 on curve2.This value is then used back in the Dynamic model to find the actual value of h. If this value of h is within the permissible error, the iteration stops. Else a new

value of C is computed from this value of h, and a new value of F is obtained. The iteration proceeds untill h for the Dynamic model is obtained within the error limits set.

The successive surfaces generated by the dynamic model, for various values of speed and feed are shown in fig 3.3 on page 27. The surface finish and tolerance is calculated for each surface. This principle can be applied to the total model (general purpose and machine specific). As more refined models are developed, the model will predict the surface finish and tolerance more accurately.

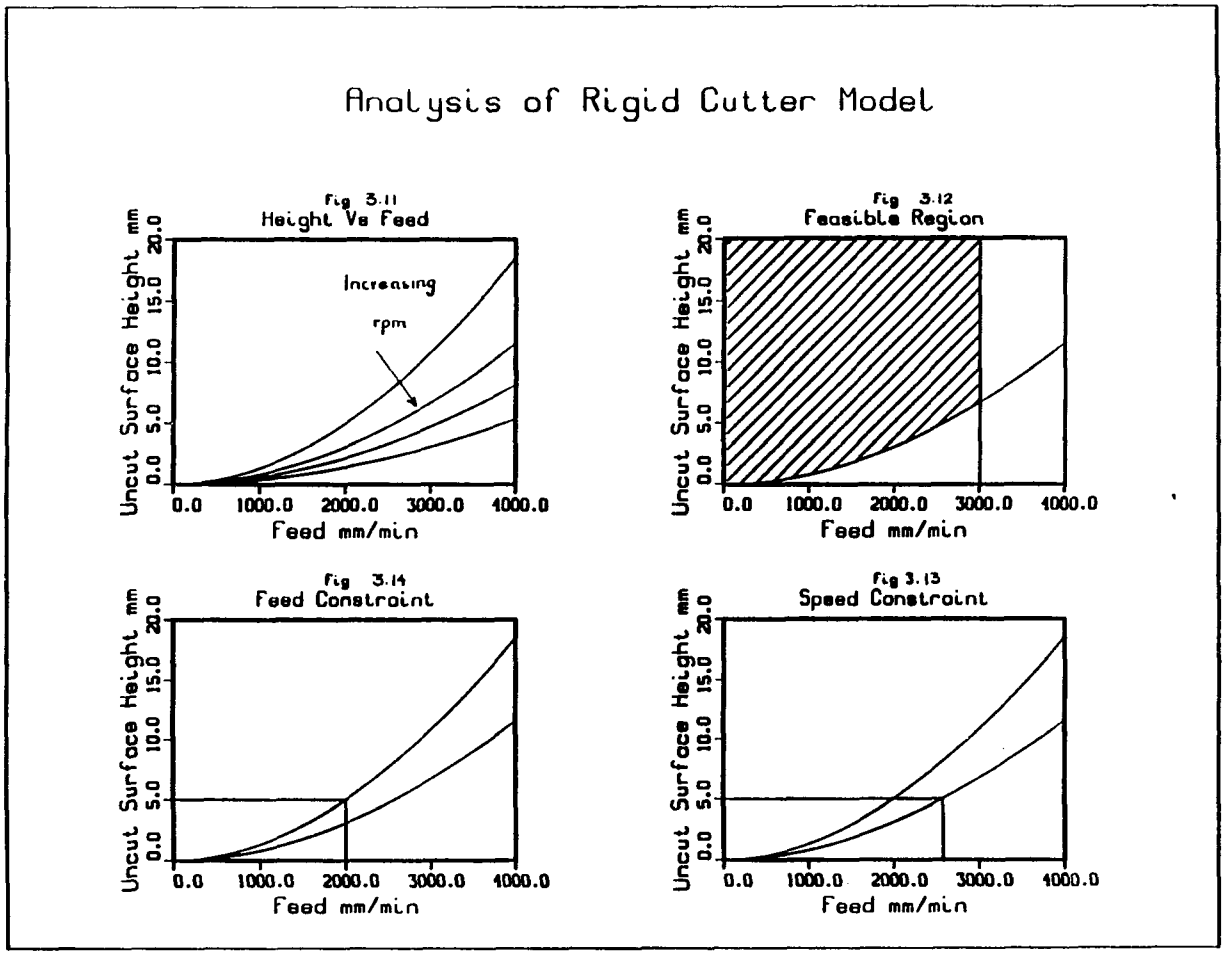

Fig 3.1 Analysis of Rigid Cutter Model

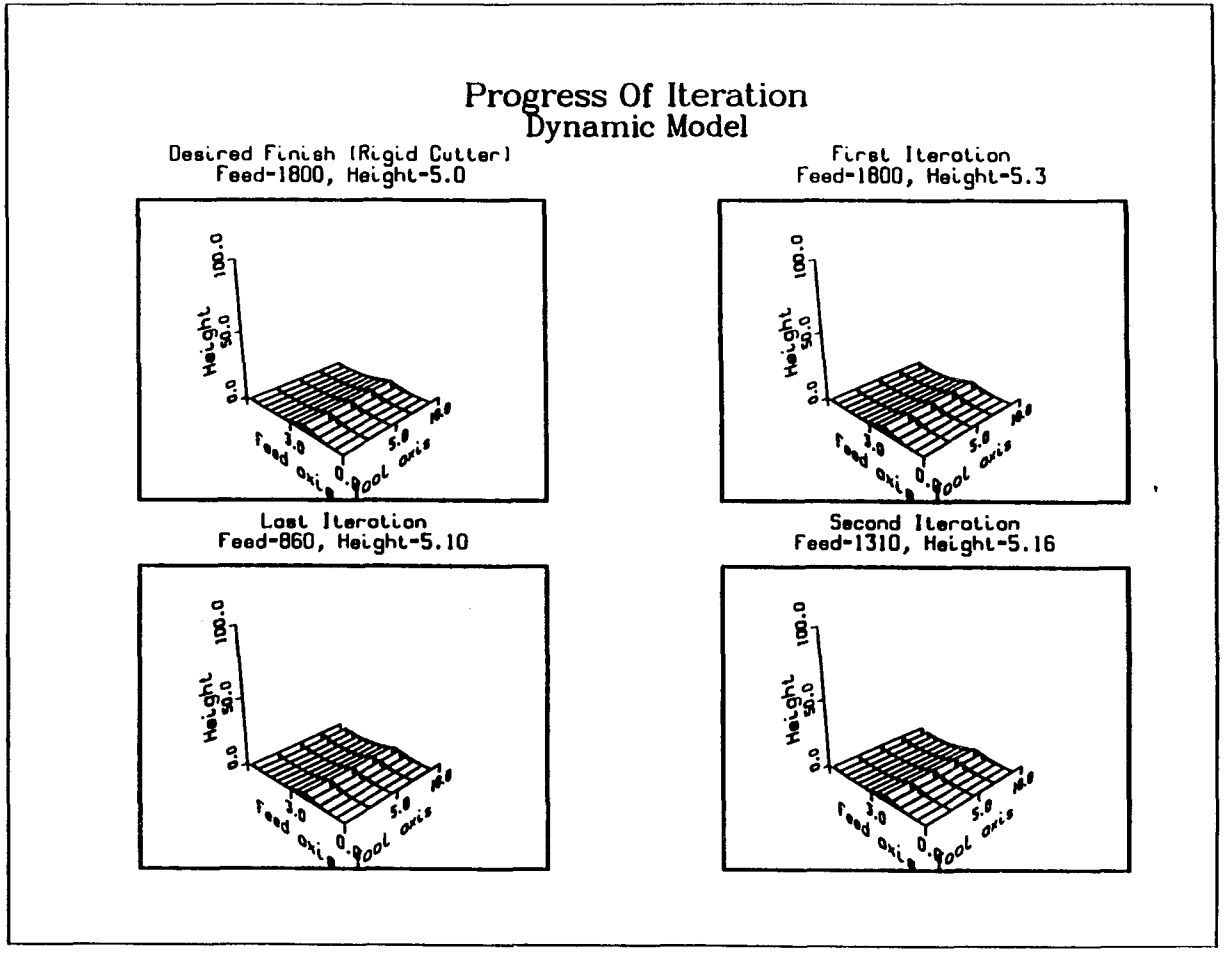

Fig 3.3 Progress of iteration

CHAPTER 4

RIGID CUTTER MODEL

The rigid tool-rigid work piece model, as the name suggests, assumes that the cutting tool is rigid and not subject to deflection. One revolution of the cutter is divided into a number of discrete time steps. The axial depth of cut is divided into a number of discrete levels or slices. The position of every tooth, at every level, at every time step, is then calculated and stored in a two 3-D arrays: one giving the X coordinate and the other array giving the Y coordinate. The coordinate system is as shown in fig 4.1.

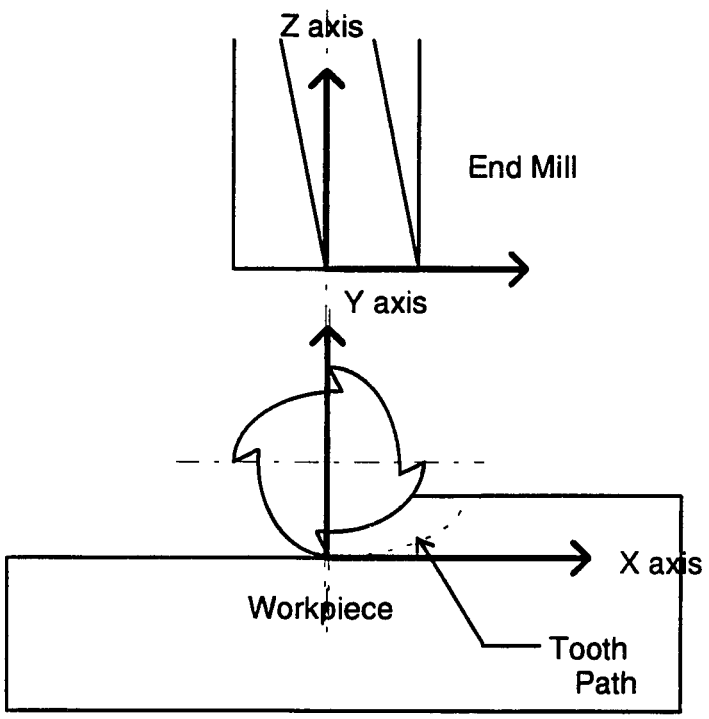

Fig 4.1 Coordinate system

These arrays are then analyzed to give the uncut surface heights at every level and at discrete distances along the feed direction. The surface thus generated can then be plotted as well as analyzed for surface roughness and tolerance.

4.1 Generation of the position arrays

The angular position of every tooth relative to the cutter axis is calculated as shown in fig 4.2

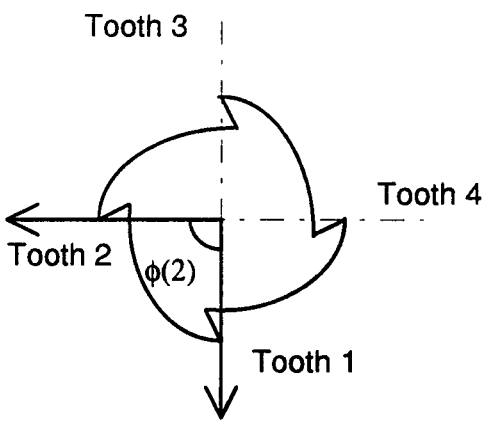

Fig 4.2 Tooth positions

$$\phi(i) = -\frac{2\pi}{T}(i-1) \qquad (4.1)$$

where i is the tooth number and T is the number of teeth.

The first tooth will therefore have 0 angle w.r.t. cutter axis.

The axial depth at any level j is calculated as under

$$\Delta z = \frac{d_a}{N_l}$$

$$z(j) = (j-1)\,\Delta z \qquad (4.2)$$

where d_a is the axial depth and N_l is the number of levels chosen

The time at any time step k is given by

$$\Delta t = \frac{60}{rpm \cdot T_n}$$

$$t(k) = (k-1)\,\Delta t \qquad (4.3)$$

where T_n is the number of time steps chosen

The angular position of the cutter at any time step k is given by

$$\theta(k) = \frac{2\pi(k-1)}{T_n} \qquad (4.4)$$

The angular position of any tooth i at any level j with respect to the cutter, changes due to the helix angle. This is given by

$$\beta(j) = z(j)\frac{2\tan(\alpha)}{D_c} \qquad (4.5)$$

where α is the helix angle of the cutter and D_c is the cutter diameter.

The angular position of any tooth i at any level j and at any time step k, is therefore,

$$\gamma(i,j,k)=\varphi(i) + \beta(j) + \theta(k) \qquad (4.6)$$

Therefore, the X and Y coordinates of any tooth i, at any level j, at any time interval k, are given by

$$X(i,j,k) = \frac{F \cdot t(k)}{60} + \frac{D_c \cdot \sin(\gamma(i,j,k))}{2} \qquad (4.7)$$

$$Y(i,j,k) = \frac{D_c}{2} \cdot (1 - \cos(\gamma(i,j,k)) \qquad (4.8)$$

The path traced by each tooth for one revolution is shown in fig 4.3 on page 32 and that for three revolutions is shown in fig 4.4 on page 33.

X and Y are the three dimensional arrays that are computed and represent the path of each tooth.

4.2 Calculation of uncut surface height

At every point along the feed axis and at every level along the axial depth, the uncut surface height is computed from the tooth paths. For any point at any level, an algorithm is developed to locate the two points on a tooth path, that are on either sides of it. Linear interpolation is used to find the point of intersection of the vertical from this point and a straight line joining the adjacent points on the tooth path. This vertical line is representative of material that remains uncut as the tooth sweeps over the point. This vertical height is calculated for every tooth. The minimum height among these is the final uncut surface left, after all the teeth have swept over the point. An array of these uncut surface heights is created.

The difference between the maximum and minimum uncut surface heights will give the surface finish of the generated surface. The minimum height represents the deviation of the surface from its intended position. This, therefore, gives the surface tolerance.

A plot of this surface is shown in fig 4.5 on page 35. This is the best possible surface that can be obtained using the milling operation.

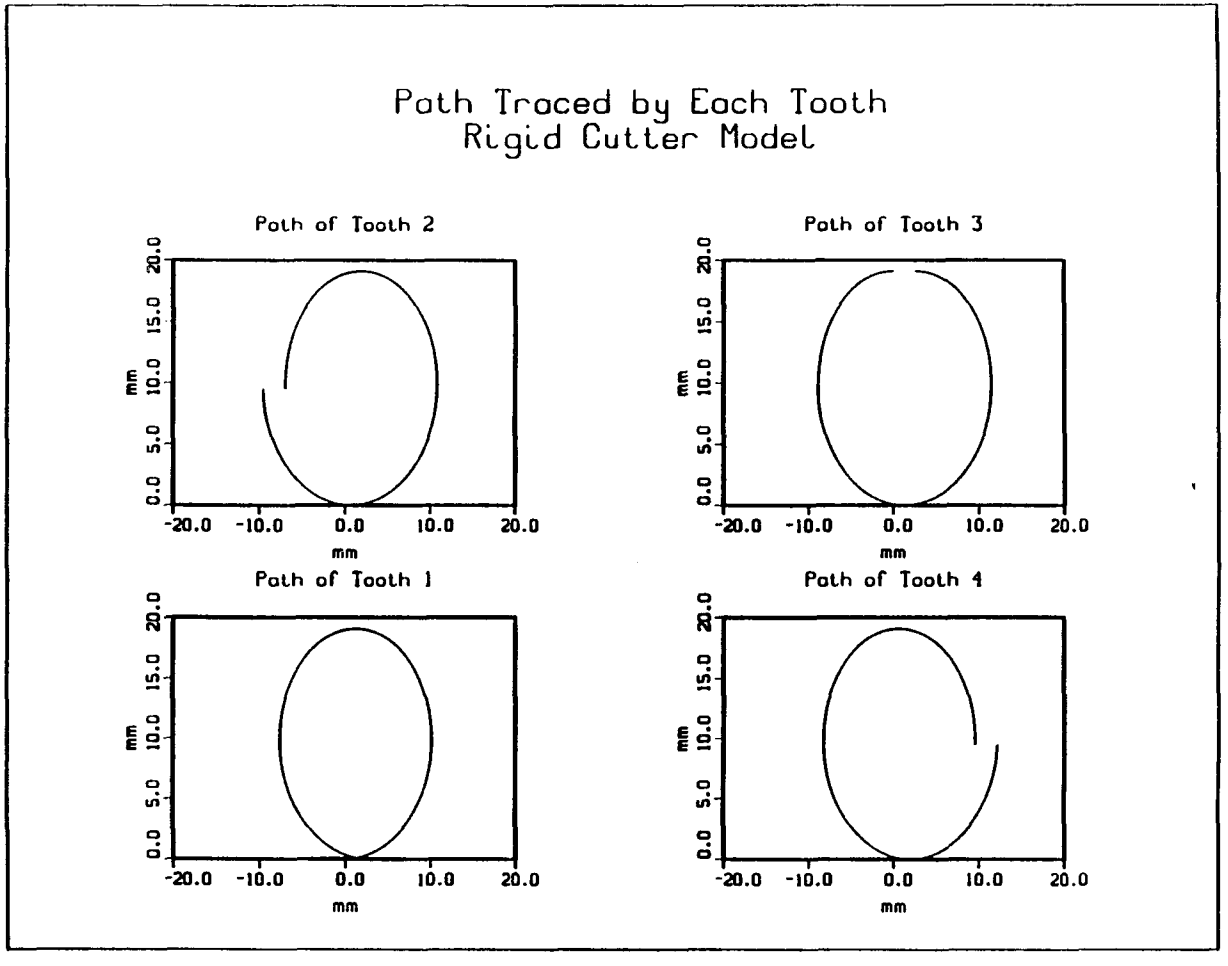

Fig 4.3 Path of each tooth, for one revolution, Rigid Cutter Model

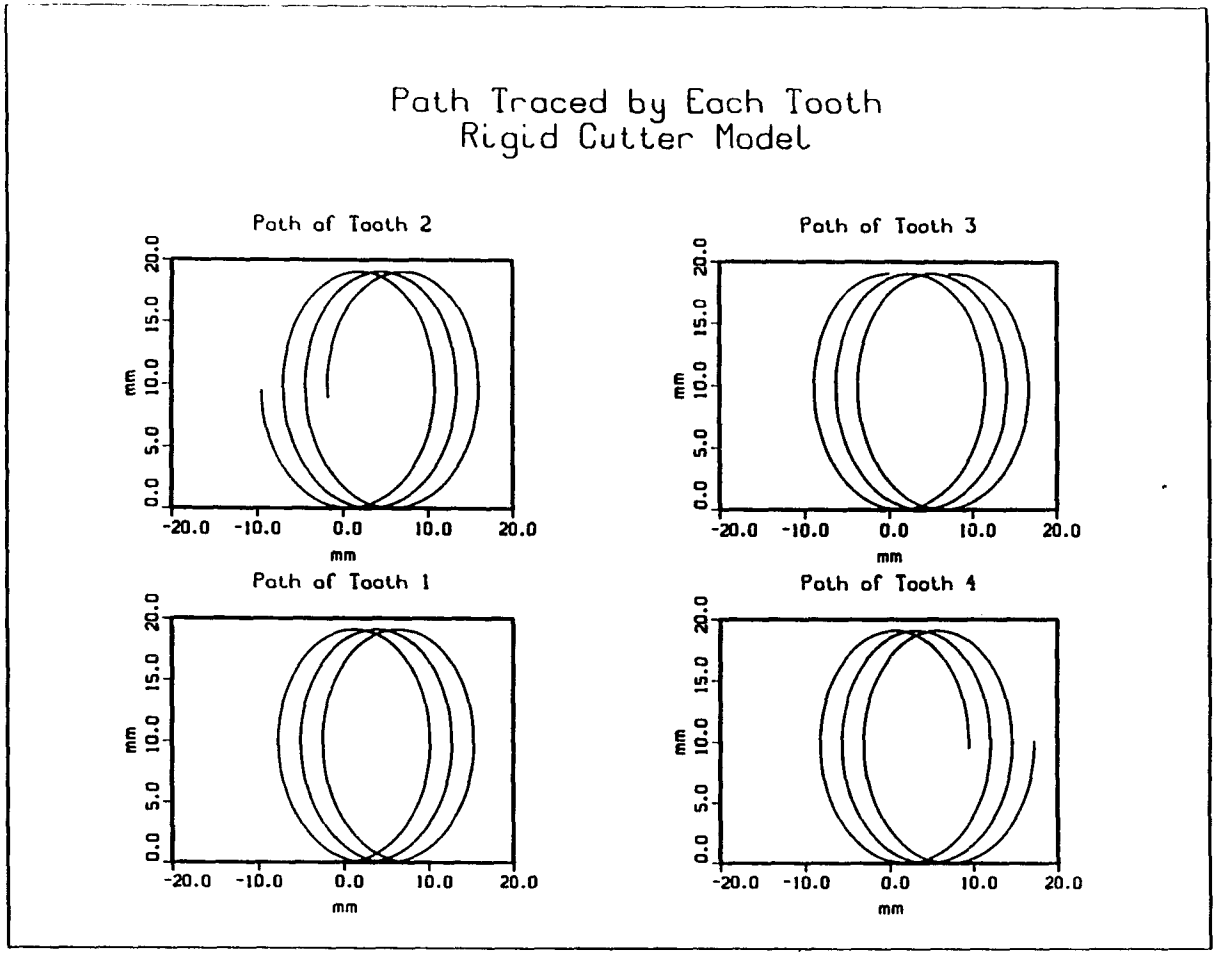

Fig 4.4 Path of each tooth, for three revolutions, Rigid Cutter Model

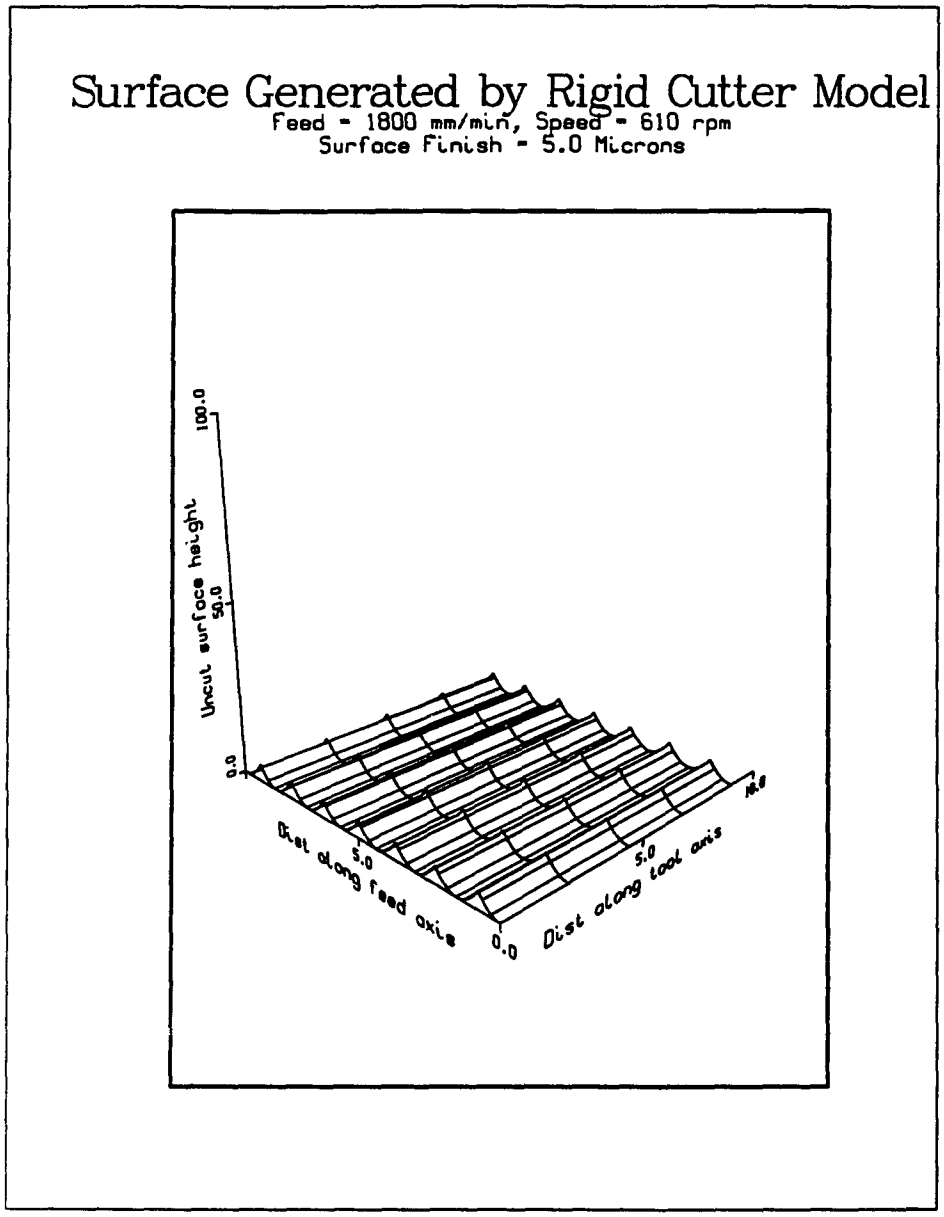

Fig 4.5 Surface generated by Rigid Cutter Model

CHAPTER 5

MODELING THE MILLING FORCES

It is necessary to model the forces involved in the milling operation, in order to build any milling model. As can be seen from the classification of various models, it is primarily the manner in which the force is modeled that sets one apart from the others. The models that use instantaneous force in their computation, basically discretize the force in time and space, by considering the end mill to be divided into a number of slices along its axis for the given radial depth of cut. Each slice is then analyzed, at any instant in time, for the cutting forces involved. The effect of these forces on the total system is then summed up.

It is interesting to note that force modeling for up milling and down milling cannot be done in the same manner because the force directions change. This is explained in detail in the section on axial force distribution. Most of the researchers have modeled the down milling situation. The up milling situation is considered here.

5.1 Force analysis for each slice

At any given time step, the cutting action of every tooth gives rise to a resultant cutting force on that tooth. This force can be resolved into two components, one tangential and another radial to the diameter of the cutter. The tangential cutting force twists the cutter and is responsible for the cutting torque. These forces acting on a slice, for the up milling situation, when the tooth is at an angle ϕ w.r.t. the chosen Y axis, are shown in fig 5.1.

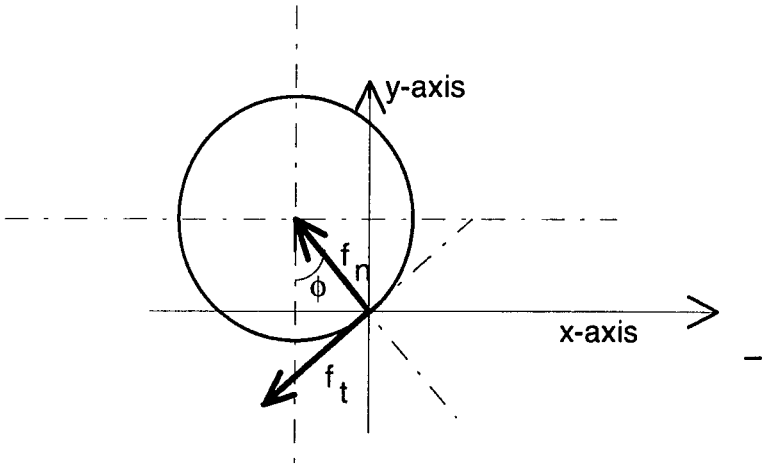

Fig 5.1 Milling forces

The forces resolved along the X axis and Y axis are as under

$$f_x = - f_n \sin \phi - f_t \cos \phi \quad (5.1)$$

$$f_y = f_n \cos \phi - f_t \sin \phi \quad (5.2)$$

5.2 Computation of normal and tangential forces

The single point orthogonal cutting model is used to compute the normal and tangential forces on any slice at any time step. The orthogonal cutting model predicts the normal and tangential forces to be proportional to the instantaneous chip thickness and width of the chip. In this case, the chip width is the width of the cutter slice, and the chip thickness varies with the feed per tooth and with the angle ϕ the tooth makes with the Y axis. The equation for the normal and tangential forces are, therefore:

$$f_n = k_{sn} \Delta z f_t \sin \phi \quad (5.3)$$

$$f_t = k_{st} \Delta z f_t \sin \phi \quad (5.4)$$

Where

k_{sn} = the force constant for the normal force,

K

k_{st} = the force constant for the tangential force.

f_t = feed per tooth

The force equations then become

$$f_x = - k_{sn} \sin \phi \sin \phi \; - \; k_{st} \cos \phi \sin \phi \qquad (5.5)$$

$$f_y = k_{sn} \cos \phi \sin \phi \; - \; k_{st} \sin \phi \sin \phi \qquad (5.6)$$

5.3 Computation of the force constants

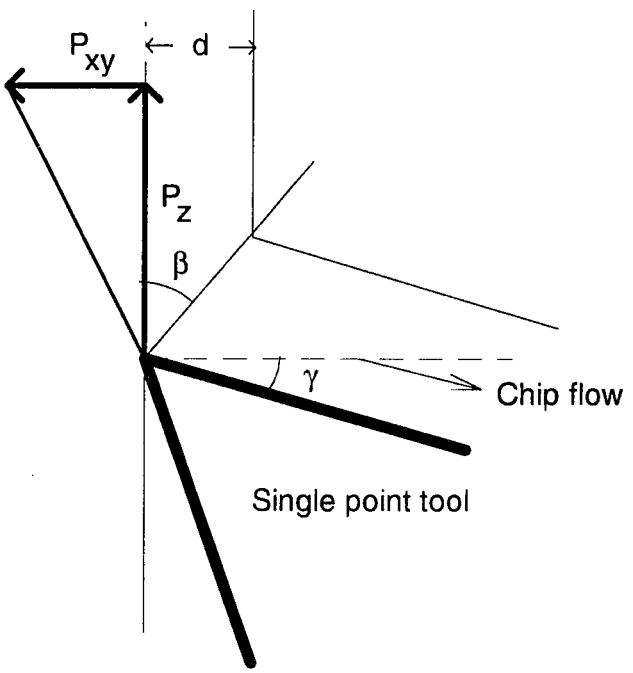

Fig 5.2 Single point orthogonal cutting model

The single point orthogonal cutting model is used to compute the cutting force constants. While there are a number of theories predicting the force constants from various material properties

and cutting conditions, the variables that were more relevant and more general in nature, were selected. The single point orthogonal cutting model is shown in fig 5.2.

The forces normal and parallel to the cutting velocity are given by

$$P_{xy} = \tau dw \frac{\sin(\eta - \gamma)}{\sin\beta \cos(\beta + \eta - \gamma)} \tag{5.7}$$

$$P_z = \tau dw \frac{\cos(\eta - \gamma)}{\sin\beta \cos(\beta + \eta - \gamma)} \tag{5.8}$$

where

τ = the shear stress at the shear plane

d = the chip thickness

w = the chip width

η = the friction angle for the given workpiece/material combination

β = the angle of the shear plane

γ = the rake angle of the cutting tool.

This model is applied to a milling cutter slice, for a particular tooth with a difference that the chip thickness varies with the angle of rotation.

The force constants are, therefore, given by the equations:

$$k_{sn} = \tau \frac{\sin(\eta - \gamma)}{\sin\beta \cos(\beta + \eta - \gamma)} \tag{5.9}$$

$$k_{st} = \tau \frac{\cos(\eta - \gamma)}{\sin\beta \cos(\beta + \eta - \gamma)} \tag{5.10}$$

There are, again, various theories to predict these variables. Equation for predicting β is taken from [15] and is given as under

$$\beta = \frac{1}{2}\sin^{-1}\left[2\frac{\sigma_{ys}}{\sigma_{ut}}\cos\left(\frac{\pi}{4} - \frac{\gamma}{2}\right)\sin\left(\frac{\pi}{4} + \frac{\gamma}{2}\right) - \sin\gamma\right] + \gamma \tag{5.11}$$

where

σ_{ys} = the yield strength of the workpiece

σ_{ut} = the ultimate strength of the workpiece

Since the shear stress at the shear plane is severe and causes the material to flow, it is taken to be 1.5 times the yield shear stress. The shear stress at the shear plane is, therefore, given by

$$\tau = 1.5\tau_{ys} = 1.5\frac{\sigma_{ys}}{2} \tag{5.12}$$

5.4 Variation in forces with cutter rotation

As the cutter rotates, every tooth experiences forces in the X and Y directions, as it cuts the material. The above equations help us to predict these forces. In case of up milling, for any slice, the variation in the X and Y forces as a function of cutter rotation is shown on page 42. It is seen that as the cut progresses, fx goes on decreasing to a minimum and then increases, while fy increases up to a maximum and then decreases. It even changes direction, implying that as the depth of cut increases, the cutter is pulled inwards.

The point of rotation where fx and fy reach a maximum can be found by differentiating the force equations and equating them to 0

$$\frac{\partial f_x}{\partial \phi} = \frac{\partial}{\partial \phi}(-k_{sn}\sin\phi\sin\phi - k_{st}\cos\phi\sin\phi)$$

$$= 0$$

gives

$$\phi = \frac{1}{2}\tan^{-1}\left[\frac{k_{st}}{k_{sn}}\right] \text{ and } \frac{\pi}{2} \tag{5.13}$$

$$\frac{\partial f_y}{\partial \phi} = \frac{\partial}{\partial \phi}(k_{sn}\cos\phi\sin\phi - k_{st}\sin\phi\sin\phi)$$

$$= 0$$

gives $$\phi = \frac{1}{2}\tan^{-1}\frac{k_{sn}}{k_{st}} \quad \text{and} \quad \frac{\pi}{2} \tag{5.14}$$

The force f_x also goes to zero at

$$\phi = \tan^{-1}\left[\frac{k_{st}}{k_{sn}}\right], \ 0, \text{ and } \pi \tag{5.15}$$

and f_y goes to zero at

$$\phi = \tan^{-1}\left[\frac{k_{sn}}{k_{st}}\right], \ 0, \text{ and } \pi \tag{5.16}$$

It should be noted that in modeling the down milling operation, the forces in X and Y direction are given by

$$f_x = - k_{sn} \sin\phi \sin\phi + k_{st} \cos\phi \sin\phi \tag{5.17}$$

$$f_y = k_{sn} \cos\phi \sin\phi + k_{st} \sin\phi \sin\phi \tag{5.18}$$

which interchanges the maxima for x and y

5.5 Force distribution along the axis of the cutter

If we consider a cutter with a left hand helix, i.e. α being negative, then the tooth position of every slice, starting from the bottom of the cut, will lag the bottom slice by an angle $\frac{2\tan\alpha\,\Delta z}{D_c}$. Subsequently, the force on the slice will be given by the same graph, at a point $\frac{2\tan\alpha\,\Delta z}{D_c}$ behind the force on the preceding slice. Therefore at any time the force distribution along the axis of the cutter will be given by a window on the graph, whose width is given by $\frac{2\tan\alpha\, d_a}{D_c}$.

As the cut progresses, the force distribution can be represented by a window of predetermined width moving across the graph. This is important in further modeling the milling operation as it has great impact on the way the deflections and dynamic displacements are modeled.

5.6 Analysis

If we consider the case of Aluminum 7075 T6, computing as above, the $\frac{k_{sn}}{k_{st}}$ ratio works out to be 0.5 for the up milling situation, and thus the force f_x has a minimum at 148.3^0 and a maximum at 90^0 . And, for f_y, the minimum occurs at 90^0 and the maximum at 13.3^0 . The f_x and f_y forces will go to zero at 116.6^0 and 26.6^0 respectively.

Considering a cutter of diameter 25.4 mm (1"), at a radial depth of cut of 1.35 mm itself, the angle of immersion of the tooth is such that f_y changes direction. The x force distribution along the cutter axis, in case of down milling and y force distribution along the cutter axis, in case of up milling, will now consist of + ve and - ve forces as the depth of cut increases. The resultant of these forces, with respect to the moments, will no longer fall within the cutter length. Modeling the cutter as a cantilever beam, with a single resultant force acting at a point, will lead to erroneous results. Therefore, the effect of each individual force, rather than the effect of a single resultant force is considered, in the deflection model and the dynamic model.

5.7 Experimental verification

Montgomery et al. [16] have experimentally verified the force constant for 7075 T6 Aluminum workpiece and HSS tool to be 1185 N/mm^2. The properties of Aluminum were substituted in the above equations and the value of K was calculated to be 1170 N/mm^2 which compares very well with the experimentally observed result.

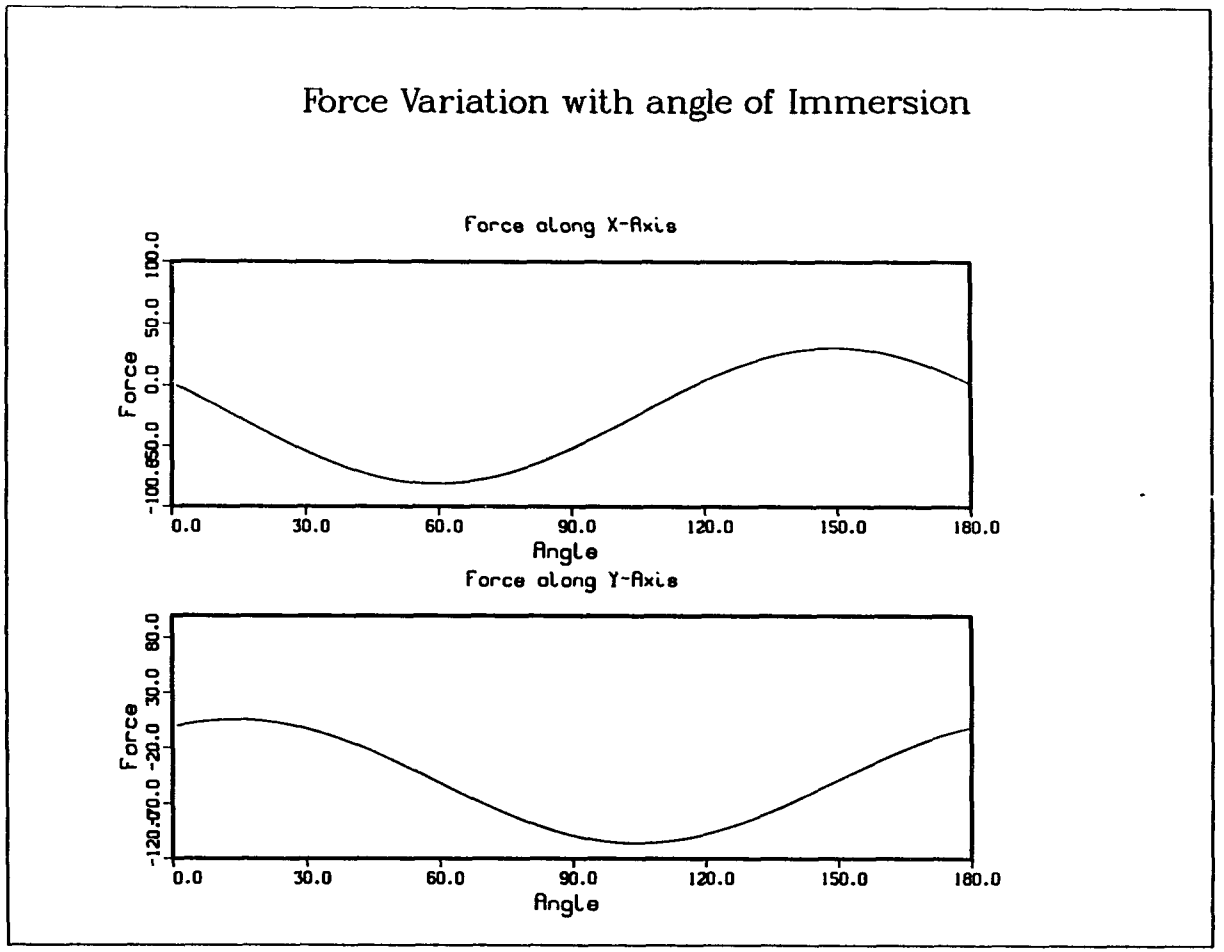

Fig 5.3 Variation of force with cutter rotation

CHAPTER 6

DEFLECTION MODEL

In this model the static deflection of the cutter is taken into account to calculate the position of every tooth, at every level and at every time step. The actual positions of the teeth differ from those given by the rigid cutter model by the amount of the static deflection. The actual position is calculated from the rigid cutter position and this is used to calculate the uncut height at each level along the feed axis. The surface thus generated is analyzed for surface finish and tolerance.

6.1 Calculation of forces

The forces in the X and Y direction at every time step are computed from equations 5.5 and 5.6.

6.2 Calculation of deflection

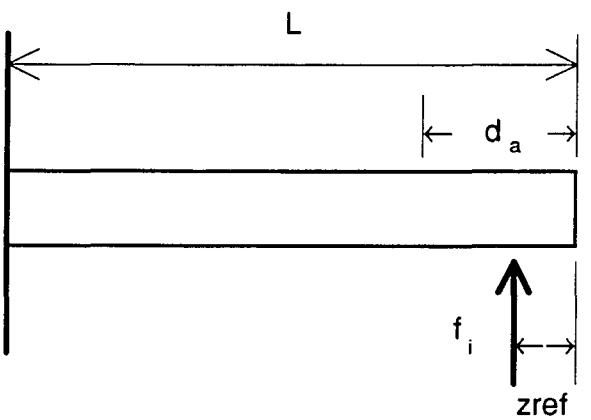

Fig 6.1 Deflection along a cantilever beam

Forces on any given slice of the cutter cause deflection of the cutter along its entire axis. Deflection along X and Y directions are computed separately. Thus, at every point along the cutter axis, deflections due to forces acting on all slices have to be summed up. The deflection at

any position at a distance z(j) along the cutter axis due to an incremental force f_i acting on the slice at a distance zref from the free end, at a time step k is then given by

For 0 < z(j) <zref

$$\delta = \frac{32f_i(L_c - zref)^2[2L_c - 3z(j) + zref]}{3E\pi D_c{}^4} \tag{6.1}$$

For zref < z(j) < L_C

$$\delta = \frac{32f_i[L_c - z(j)]^2[2L_c - 3zref + z(j)]}{3E\pi D_c{}^4} \tag{6.2}$$

where

L_C = length of the cutter

E = elastic constant of the cutter

D_C = diameter of the cutter

Deflections in X and Y axis are computed for every point along the cutter axis due to forces acting on every slice. The sum total of all these deflections at any point, give the final deflection at that point.

6.3 Calculation of position arrays

The deflection at any level j is the same for all teeth positions at that level. These deflections are then added to the theoretical positions arrays to give the actual positions arrays.

$$X_{act}(i,j,k) = X_{th}(i,j,k) + \delta x(i,j,k)$$

$$Y_{act}(i,j,k) = Y_{th}(i,j,k) + \delta y(i,j,k)$$

The path traced by each tooth for one revolution, is shown in fig 6.2 on page 46, while that for three revolutions is shown in fig 6.3 on page 47.

6.4 Calculation of uncut surface height

At every point along the feed axis and at every level along the axial depth, the uncut surface height is computed from the tooth paths. For any point at any level, an algorithm is developed to locate the two points on a tooth path, that are on either side of it. Linear interpolation is used to find the point of intersection of the vertical from this point and a straight line joining the adjacent points on the tooth path. This vertical line is representative of material that remains uncut as the tooth sweeps over the point. This vertical height is calculated for every tooth. The minimum height among these is the final uncut surface left, after all the teeth have swept over the point. An array of these uncut surface heights is created.

The difference between the maximum and minimum uncut surface heights will give the surface finish of the generated surface. The minimum height represents the deviation of the surface from its intended position. This therefore gives the surface tolerance.

A plot of this surface is shown in fig 6.4 on page 48.

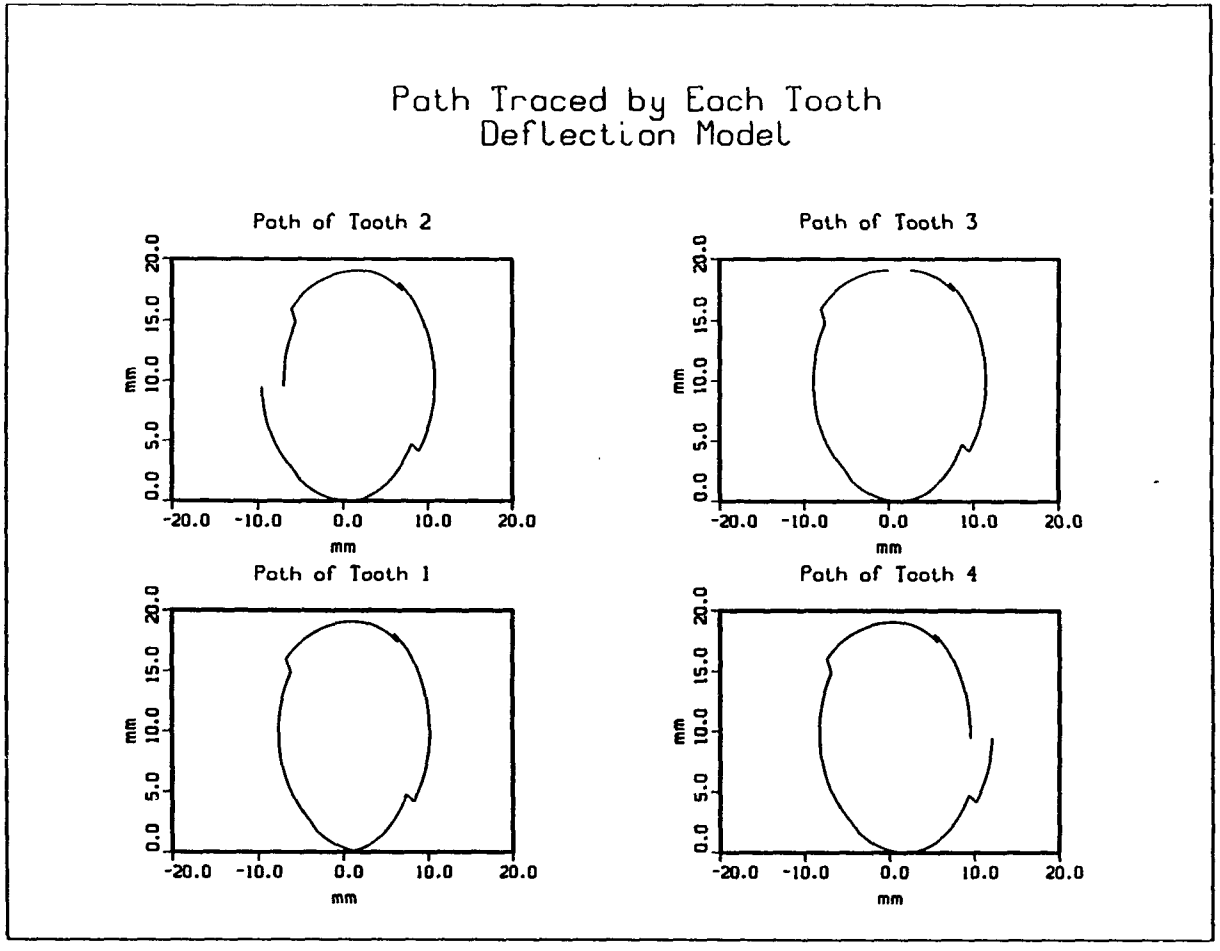

Fig 6.2 Path of each tooth, for one revolution, Deflection Model

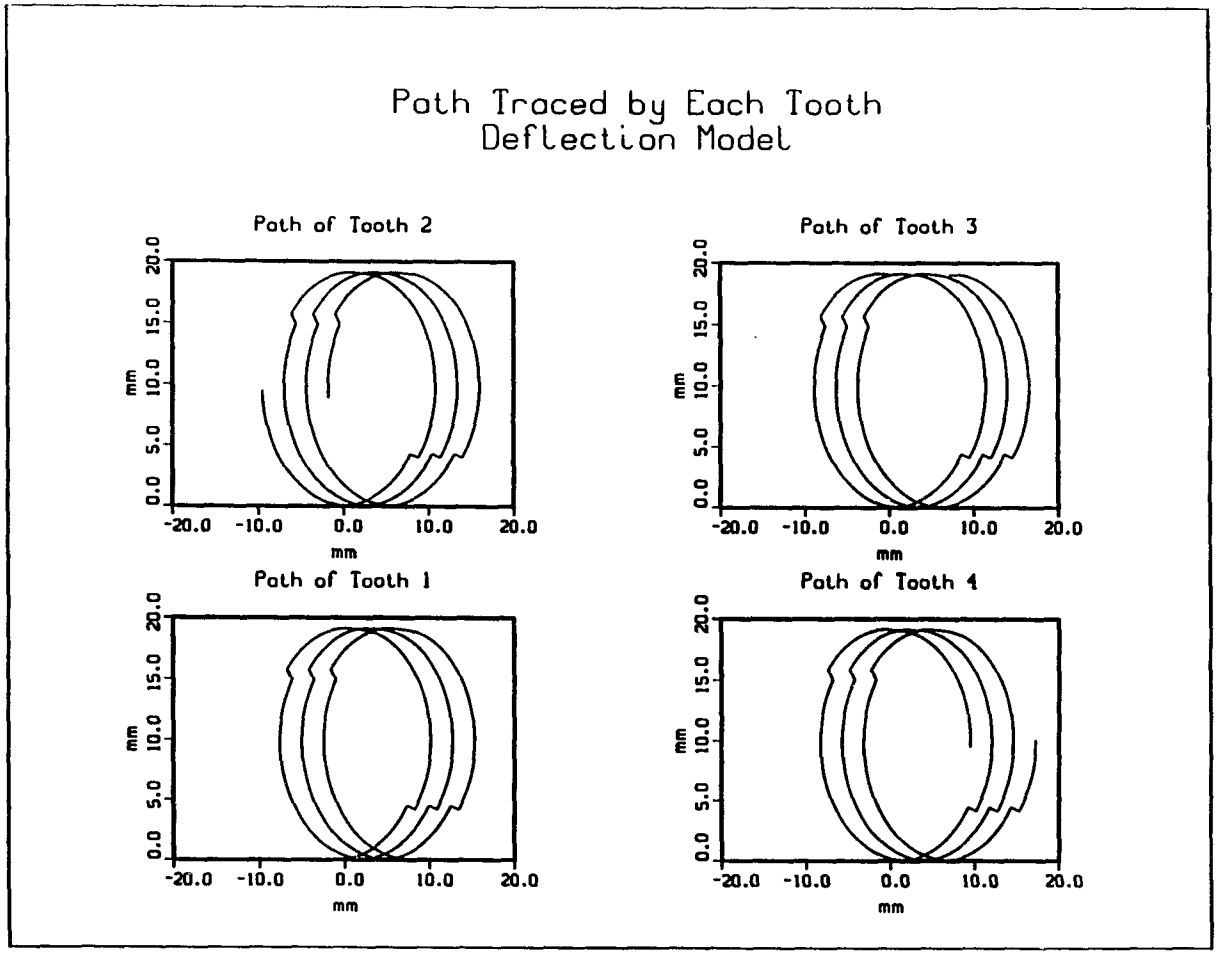

Fig 6.3 Path of each tooth, for three revolutions, Deflection Model

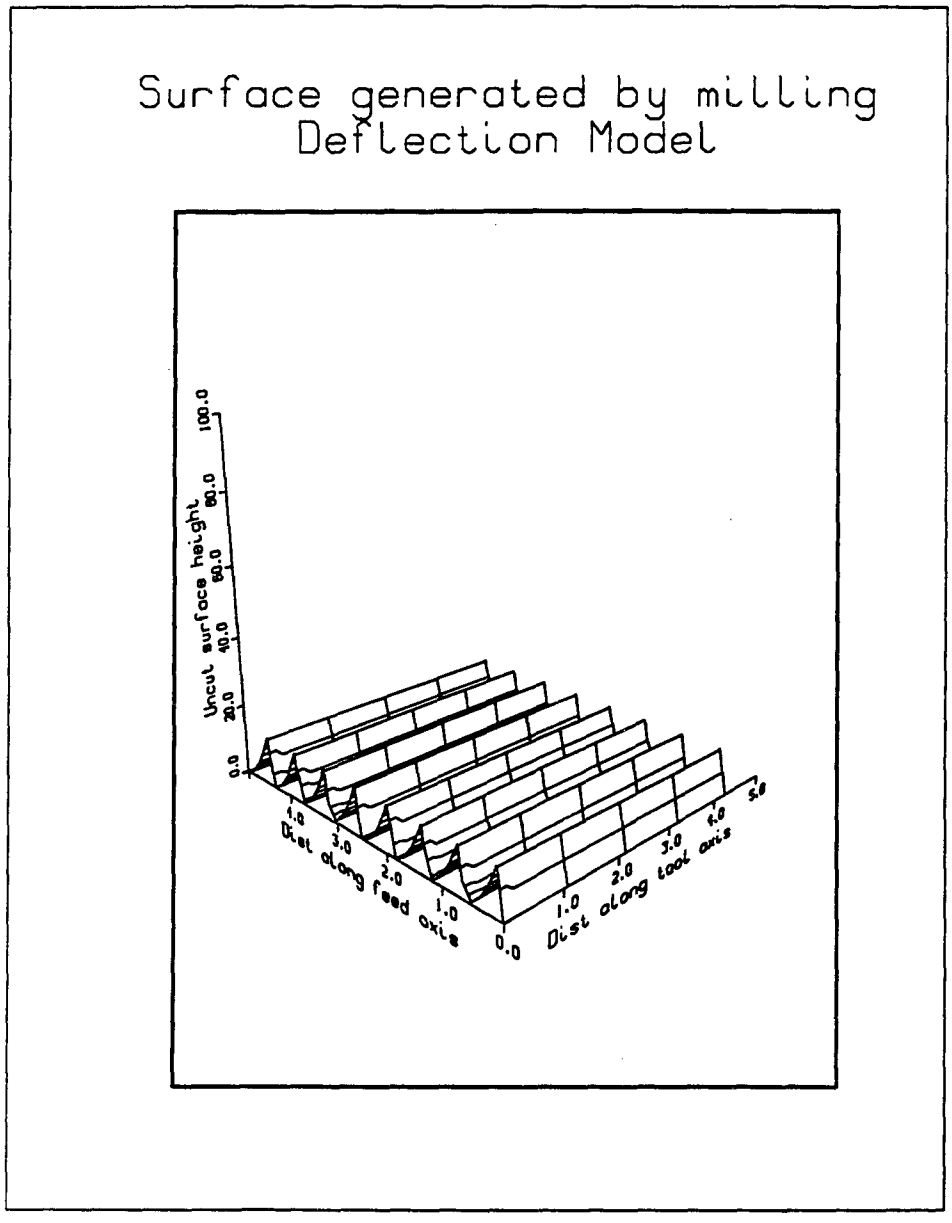

Fig 6.4 Surface generated by Deflection Model

CHAPTER 7

DYNAMIC MODEL

In this model, the time response of the deflecting force on the cutter is taken into account while calculating its deflection. The deflection model assumes the deflection of the cutter due to the cutting force to be instantaneous and computes it as static deflection. This is approximately true for low speeds and feeds. However, as the feed and speed increases, the cutter moves to a new position, before its is fully deflected.

7.1 Governing equations of motion

The position of the cutter in the time domain can be found by modeling the cutter as a mass-spring-damper system with two degrees of freedom. The motion along the feed axis constitutes the X axis and the motion perpendicular to it, the Y axis as shown in fig 7.1

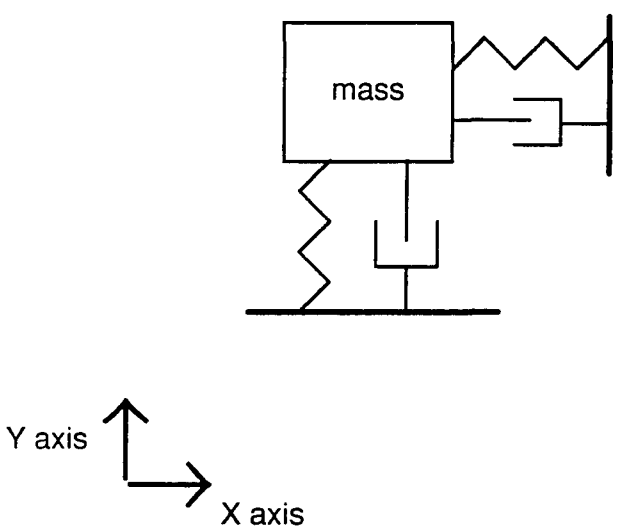

Fig 7.1 Mass, spring, damper system for dynamic model

The equations of motion in each axis are,

$$m\frac{\partial^2 x}{\partial t^2}+c\frac{\partial x}{\partial t}+kx=F_x \tag{7.1}$$

$$m\frac{\partial^2 y}{\partial t^2}+c\frac{\partial y}{\partial t}+ky+F_y \tag{7.2}$$

These equations can be solved numerically for every time step, as under

$$\left[\frac{\partial^2 x}{\partial t^2}\right]_n=\left[\frac{F_x-c\frac{\partial x}{\partial t}-kx}{m}\right]_n \tag{7.3}$$

$$\left[\frac{\partial x}{\partial t}\right]_{n+1}=\left[\frac{\partial x}{\partial t}\right]_n+\left[\frac{\partial^2 x}{\partial t^2}\right]_n\Delta t \tag{7.4}$$

$$[x]_{n+1}=\left[\frac{\partial x}{\partial t}\right]_n+\left[(1-\beta)\left(\frac{\partial x}{\partial t}\right)_n+\beta\left(\frac{\partial x}{\partial t}\right)_{n+1}\right]\Delta t \tag{7.5}$$

and similarly for y axis

$$\left[\frac{\partial^2 y}{\partial t^2}\right]_n = \left[\frac{F_y - c\frac{\partial y}{\partial t} - ky}{m}\right]_n$$

$$\left[\frac{\partial y}{\partial t}\right]_{n+1} = \left[\frac{\partial y}{\partial t}\right]_n + \left[\frac{\partial^2 y}{\partial t^2}\right]_n \Delta t$$

$$[y]_{n+1} = [y]_n + \left[(1-\beta)\left(\frac{\partial y}{\partial t}\right)_n + \beta\left(\frac{\partial y}{\partial t}\right)_{n+1}\right]\Delta t$$

where

m = mass of the cutter

k = spring constant for the cutter

c = damping coefficient

x = displacement in x direction

y = displacement in y direction

n = time step number

β = constant, >0.5 and <1.0

Δt = time step

F_x = force in the x- direction

F_y = force in the y- direction

The initial conditions for solving these equations are

x and y = 0 at t = 0 ;

$$\frac{\partial x}{\partial t} \text{ and } \frac{\partial y}{\partial t} \text{ are 0 at } t = 0 ;$$

The time step has to be very small, as compared to the deflection model, if the above equations are to give any meaningful displacements. Typically, Δt has to be in the region of 10-20 micro-seconds.

7.2 Calculation of spring constant

The spring constant for the system is calculated assuming the cutter to be a cantilever, with an equivalent force acting at a distance $\frac{d_a}{2}$ of from the free end of the cutter as shown in fig 7.2.

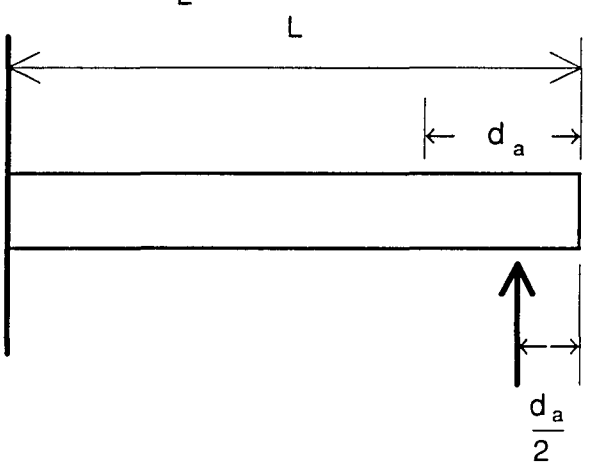

Fig 7.2 Force location for computation of spring constant

This gives the following equations

$$k = \frac{3E\pi D^4}{64\left(L - \frac{d_a}{2}\right)^3} \qquad (7.6)$$

7.3 Calculation of equivalent force

The force acting on any slice of the cutter can be moved to the center of the axial depth of cut, and replaced by a force and a moment. If the cutter is modeled as a cantilever beam, this moment can be assumed to cause some deflection. The moment can then be replaced by an equivalent force that causes the same deflection at that point. Deflection caused by a moment acting at a point midway at the axial depth of cut is given by

$$\delta_m = \frac{M\left[L - \frac{d_a}{2}\right]^2}{2EI} \tag{7.7}$$

where

M = moment

L = length of the cutter

I = moment of inertia

While deflection caused by a force acting at the same point is

$$\delta_f = \frac{f\left[L - \frac{d_a}{2}\right]^3}{3EI} \tag{7.8}$$

Equating the two deflections the force f_e equivalent to the moment M is given by

$$f_e = \frac{3M}{2\left[I - \frac{d_a}{2}\right]} \tag{7.9}$$

A force f acting on a slice at a distance of z from the free end of the cutter, produces a moment of $-f\left[z - \frac{d_a}{2}\right]$ and, therefore, the equivalent force f_e when f is shifted to $\frac{d_a}{2}$ is given by

$$f_e = \frac{-3f\left[z - \frac{d_a}{2}\right]}{2\left[L - \frac{d_a}{2}\right]} \qquad (7.10)$$

All forces on all cutter slices are thus shifted to the midpoint of the axial depth of cut, and replaced by an equivalent force. All x and y forces are then summed up and these f_x and f_y forces are used in the equations (7.1) and (7.2)

7.4 Filtration of frequencies

The displacements given by the above numerical solutions, contain the entire range of frequencies up to $\frac{1}{2\Delta t}$. The algorithms for finding the chip thickness at a particular time step, intersections of tool paths, uncut surface height require a trend in the displacement arrays. The higher frequencies have to be filtered out, to make the algorithms robust. A digital filter is employed for this purpose. The finite impulse response (FIR) filter, filters out higher frequencies as under.

$$xf_n = \sum_{k=0}^{m} c_k x_{n-k} \qquad (7.11)$$

where xf is the filtered output of x, m is a number >1 and c_k are k coefficients. If c_k s are taken as $\frac{1}{m}$ then all frequencies above $\frac{1}{m\Delta t}$ are filtered out. As it is necessary to retain all frequencies upto the natural frequency of the cutter, m can be so chosen that all frequencies upto 120% of the natural frequencies are retained.

The natural frequency of the cutter is given by

$$f_n = \frac{1}{2\pi}\sqrt{\frac{k}{m}} \qquad (7.12)$$

where

k = cutter sfiffness

m = mass of the cutter

The value for j then has to be greater than

$$j \geq \frac{8\pi}{5\Delta t}\sqrt{\frac{m}{k}} \tag{7.13}$$

The filtered displacements are shown in fig 7.3 on page 57. These represent the cutter vibrations along each axis.

These are similar to the static displacements, with vibrations superimposed.

7.5 Calculation of cutter deflection

The filtered displacements obtained above, are however displacements at the point of application of the resultant force. For displacements at other points of the cutter, the cantilever deflection equation is used. This gives the displacement at any point z mm away from the end of the cutter as

For 0<z<cf

$$\delta = \left[\frac{2L - 3z + \frac{D_a}{2}}{2L - D_a}\right].x \tag{7.9}$$

For z> cf

$$\delta = \left[\frac{(L-z)^2}{\left(L - \frac{D_a}{2}\right)^2}\right].\left[\frac{2L - 3\frac{D_a}{2} + z}{2L - D_a}\right].x \tag{7.10}$$

where **x** is the displacement as given by the solution of the dynamic equations.

7.6 Calculation of tooth paths

The paths of every tooth are then calculated by adding the above displacements to the rigid cutter tooth path. A plot of these paths is shown in fig 7.4 on page 58 for one revolution and in fig 7.5 on page 59 for three revolutions.

7.7 Surface generation

At every point along the feed axis and at every level along the axial depth, the uncut surface height is computed from the tooth paths. These height arrays define the machined surface and a plot of this surface is show in fig 7.6 on page 60.

With the given L.H. helix angle it can be seen that while the bottom portion of each tooth reaches the desired surface to be machined, the top portion is deflected away as it reaches the surface. The resultant machined surface is positioned correctly at the bottom, but is away at the top. This is the tolerance of the machined surface. A R.H. helix angle will give the opposite effect.

Therefore, an examination of the uncut surface heights at the bottom will give us the surface finish, while that at the top will give the surface tolerance.

The iterations for the desired surface finish are done in the same way as described in Chapter 3. The surface generated through several iterations is shown in fig 3.3 on page 27.

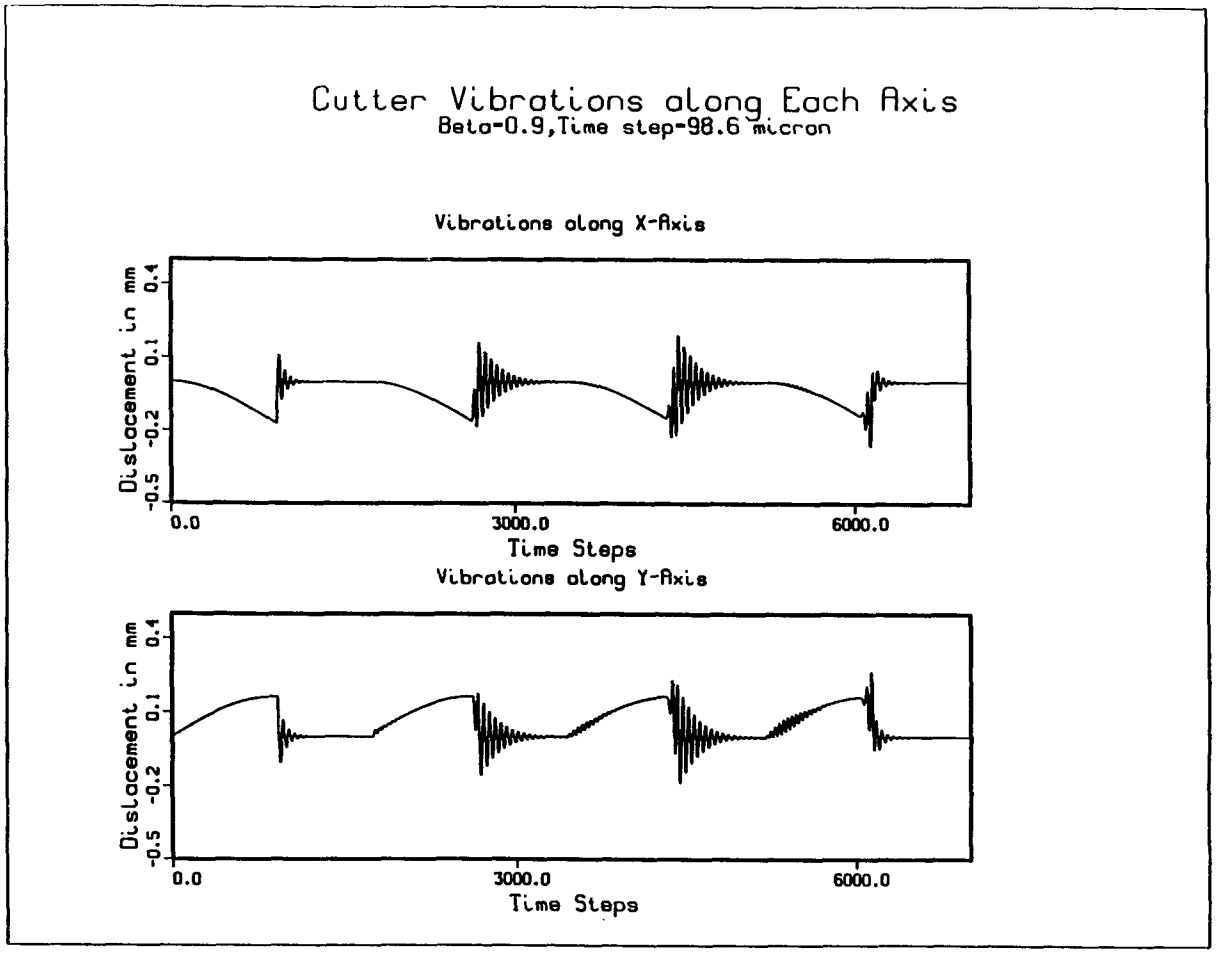

Fig 7.3 Cutter vibrations along X and Y axis

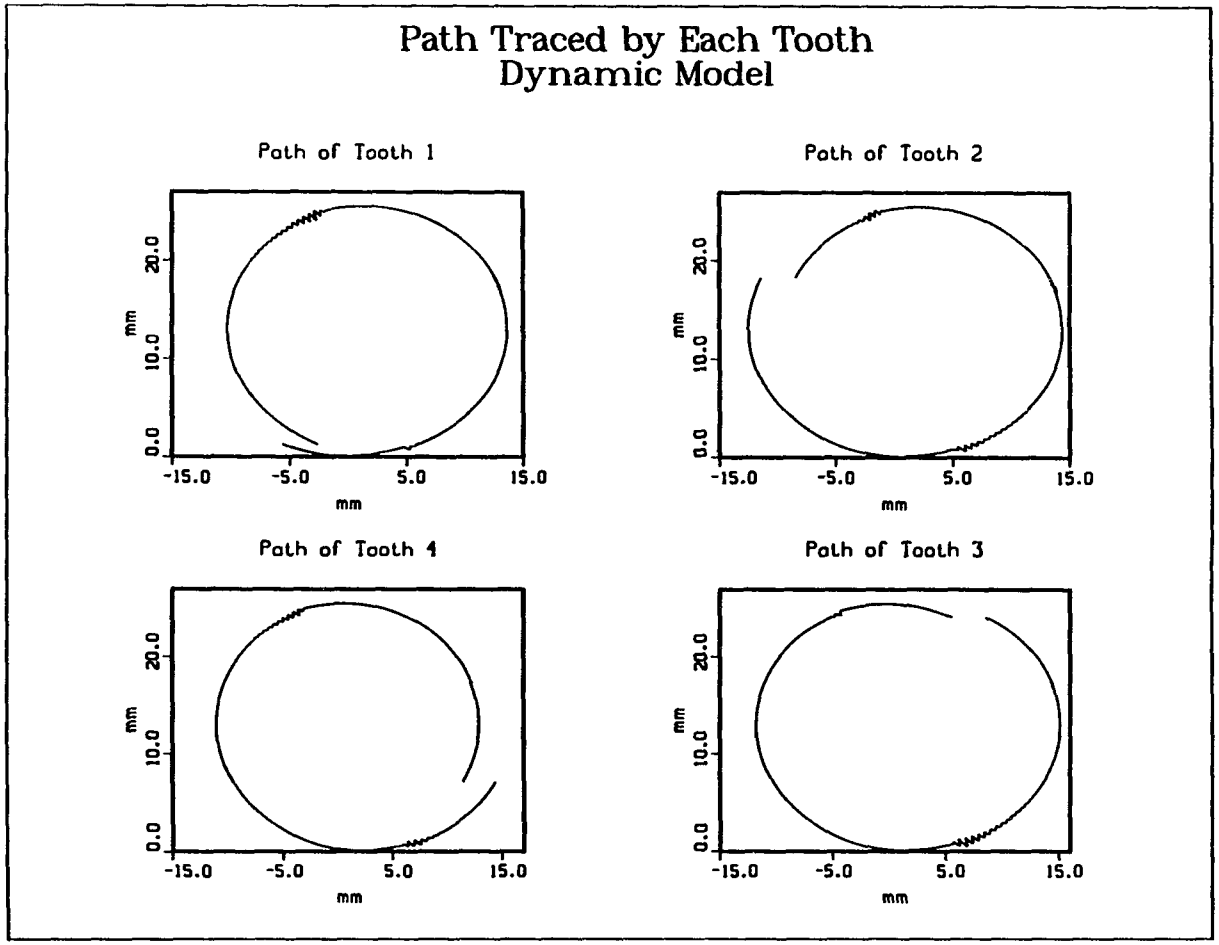

Fig 7.4 Path of each tooth, for one revolution, Dynamic Model

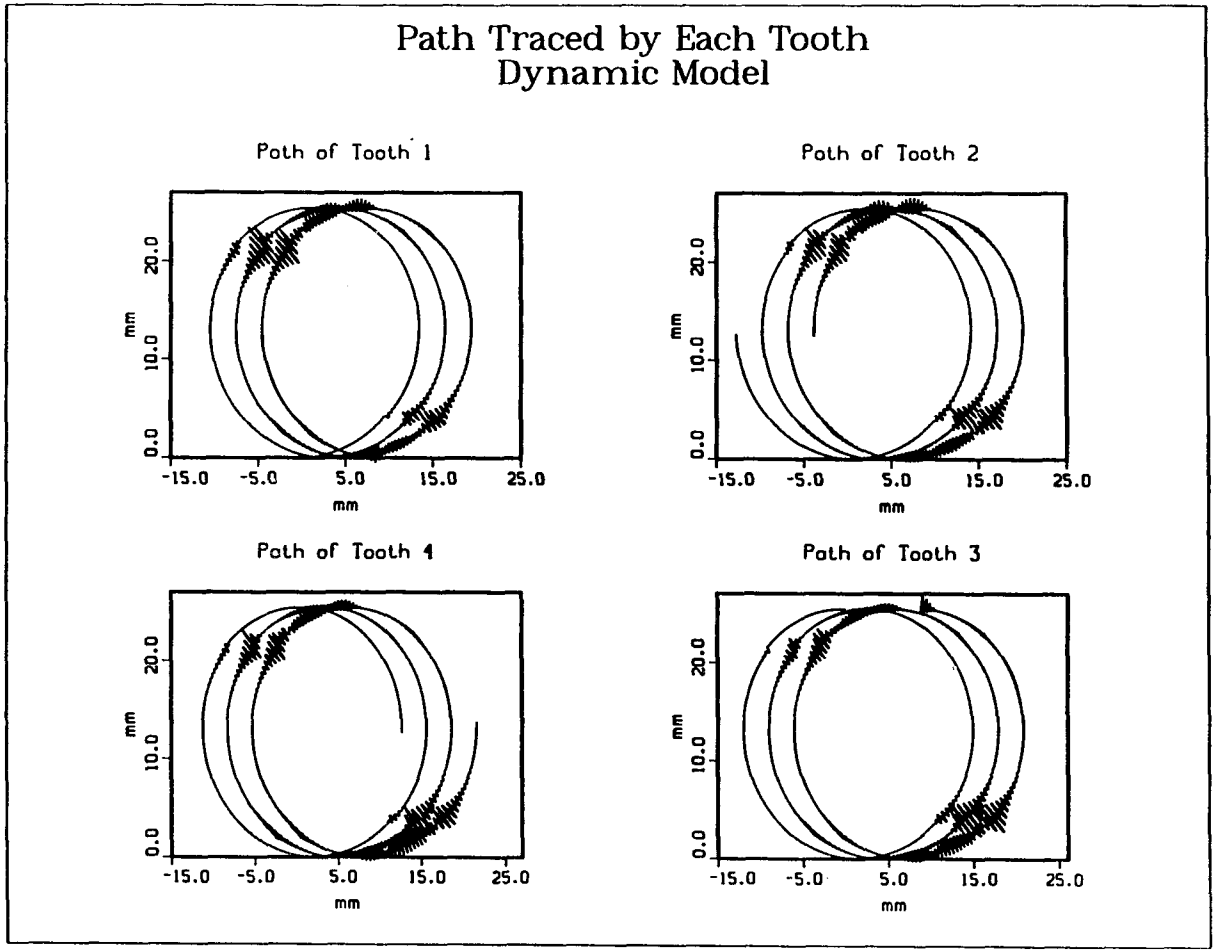

Fig 7.5 Path of each tooth, for three revolutions, Dynamic Model

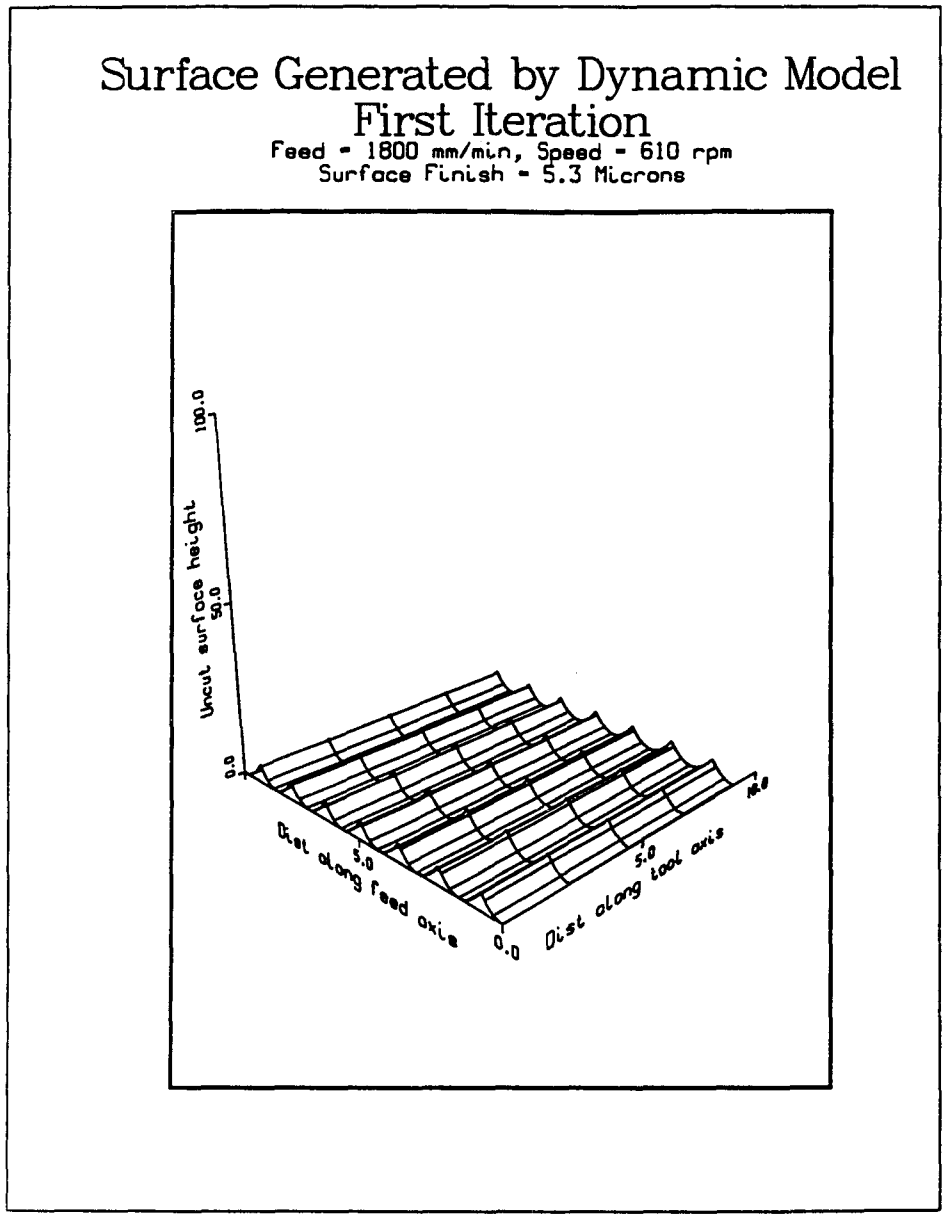

Fig 7.6 Surface generated by Dynamic Model

CHAPTER 8

FEATURE REPRESENTATION

The milling models built so far consider the case of only plain milling, with a constant radial depth of cut. In $2\frac{1}{2}$ D milling, it is often necessary to mill features, that involve variation in the radial depth of cut. It is therefore necessary to incorporate this in the milling model when predictions in surface generated are to be made.

8.1 Features representation

As a vast variation in the features is found, it is necessary to model a general case, that can be applied to a feature either directly or by converting the feature to an equivalent one. The approach adapted here, is to model the feature as a cubic curve, with the surface generated by milling as a plain surface. This representation is as shown below in fig 8.1

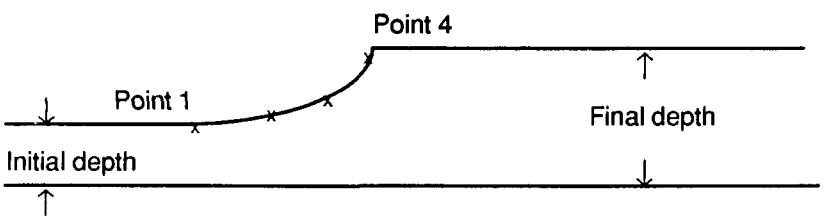

Fig 8.1 PC curve representation for a feature

The feature between the initial and final depths of cuts is modeled as a parametric cubic (PC) curve with four points on the curve being specified. As the cubic form is a general one, arcs, straight lines, steps or any form can be closely represented. Manipulation of the cubic representation for chip thickness calculations is also easier. Any geometry other than that

requiring a flat final finish can be converted into an equivalent geometry in the above form. Most of the situations that occur in $2\frac{1}{2}$ D milling can thus be represented.

The dynamic model is now modified to take into account the above geometry. The chip thickness for every tooth is not only computed with respect to path of the previous tooth, but also with respect to the feature, as represented by the above parametric cubic curve. The line from the cutter center and the present tooth position is represented as a parametric line, and the intersection of the two lines is computed. The parameters for both the curves is allowed to vary from 0 to 1. Therefore if the parameters of the intersection point lie within 0 and 1, it is a valid intersection for calculation of the chip thickness. The minimum of the two chip thicknesses calculated is taken for the computation of the cutting force.

A test case was run with an initial depth of cut of 2 mm and a final depth of cut of 5 mm. A step was incorporated in between. The plot of vibrations induced when a plain cut of 2 mm is taken is shown in fig 8.2 on page 65. This plot gets modified as the step is introduced. This plot is shown is fig 8.3 on page 66. It can be seen that the first tooth cuts in the normal way. The second tooth encounters the step and due to this its vibrations and displacement increase. The third tooth too encounters the step and its vibrations and displacement also show a similar change. The fourth tooth now encounters only the plain increased step of 5 mm and its vibration and displacement pattern is similar to the first tooth with higher displacement as can be expected.

8.2 Experimental Verification

Cutting test were carried out on Lagun CNC Vertical Milling machine with Dynapath control, on an Aluminum 7075 T6 workpiece. HSS cutters with 4 flutes, helix angle of 30 degrees and diameters of 6.35 mm and 19.05 mm were used. Axial depth of cut was 1.0 mm and radial depth of cut was varied from 1.0 mm to 3.00 mm, incorporating a step and a curve in between. Spindle

rpm of 1007 and feed of 378.5 mm/min was used for both the cutters. The results of the experiment and the simulation are shown in table 8.1.

Table 8.1 Experimental and predicted results

Cutter Diameter (mm)	Depth of cut (mm)	Peak to Valley (microns) Measured	Predicted
6.35	1.0 plain	4.9	4.52
6.35	2.0 plain	5.0	5.55
6.35	3.0 plain	9.1	9.60
6.35	1.0 step	7.0	4.70
6.35	2.0 step	9.0	5.68
19.04	1.0 plain	10.0	8.51
19.04	2.0 plain	11.5	11.06
19.04	3.0 plain	23.0	20.20
19.04	1.0 step	10.5	10.75
19.04	2.0 step	14.5	12.90
19.04	2.0 curve	12.0	11.23

The surface profiles measured and predicted for 6.35 mm cutter with 1.0 mm plain and 2.0 mm step radial depth of cuts, are shown in fig 8.4 on page 67, while that for 1.0 mm step is shown in fig 8.5 on page 68. It can be seen that the predicted peak to valley height and surface profile agrees well with experimental results. However during the machining with 19.04 mm cutter, a lot of vibrations were observed. The vibrations damaged the surface finish and the predictions of surface profile do not match the actual one. This is shown in fig 8.5 on page 68. The vibrations could have been caused by a blunt cutter.

It was also observed during the machining of features, that vibrations were set off in the machine slides. The vibrations of the cutter will have an effect on the surface finish only if the vibration region corresponds to the region in which the tooth is generating the surface. This is explained in detail in chapter 9 on design synthesis.

8.3 Material In homogeneity

The commercial materials used in machining are never homogenous. They have inclusions and impurities that have an effect on the cutting force and ultimately the surface finish. It is necessary to build this factor into the milling model. Therefore, the force model is modified to take into account the properties of the material that is being machined at a given instant of time. For example, if cast iron has carbon inclusions, their location and size is input to the model. The force model computes the force constants for machining carbon, and when any given tooth is cutting the inclusion, the appropriate force constants are used giving the changed force.

This model modification is also useful to study the process of milling two different material slabs welded together. The vibrations imposed when Aluminum and steel blocks welded together and machined are simulated and shown on page 69.

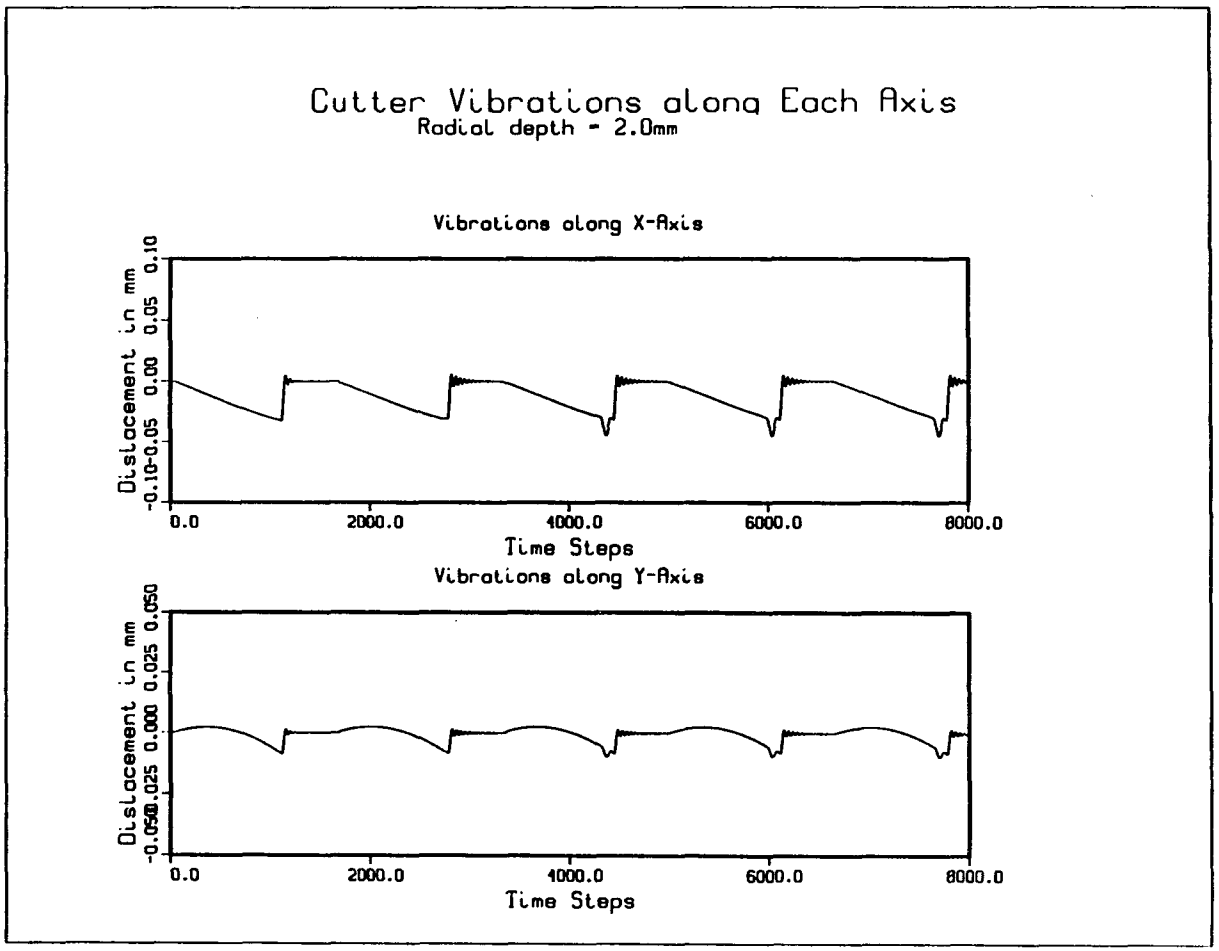

Fig 8.2 Cutter vibrations for plain cut

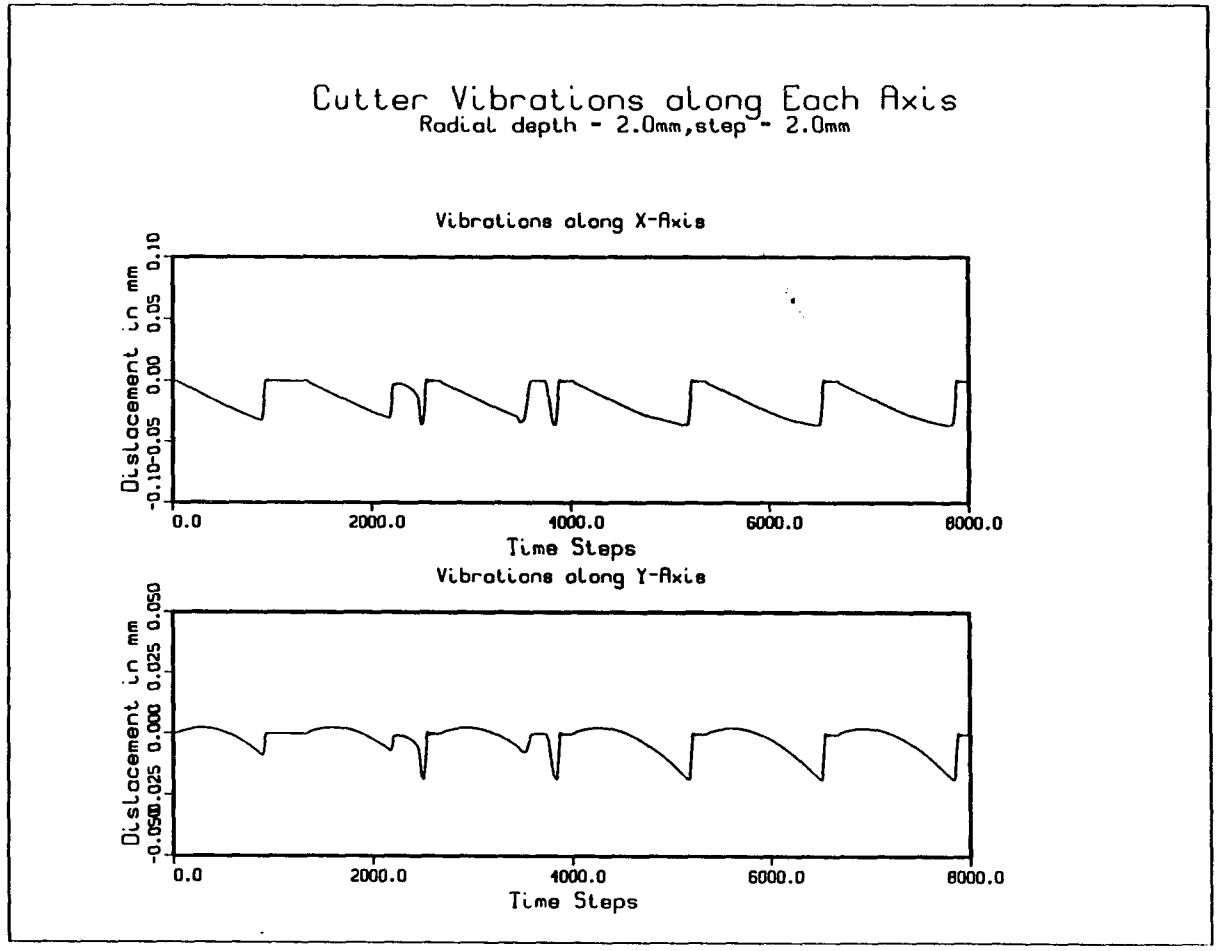

Fig 8.3 Cutter vibrations for step cut

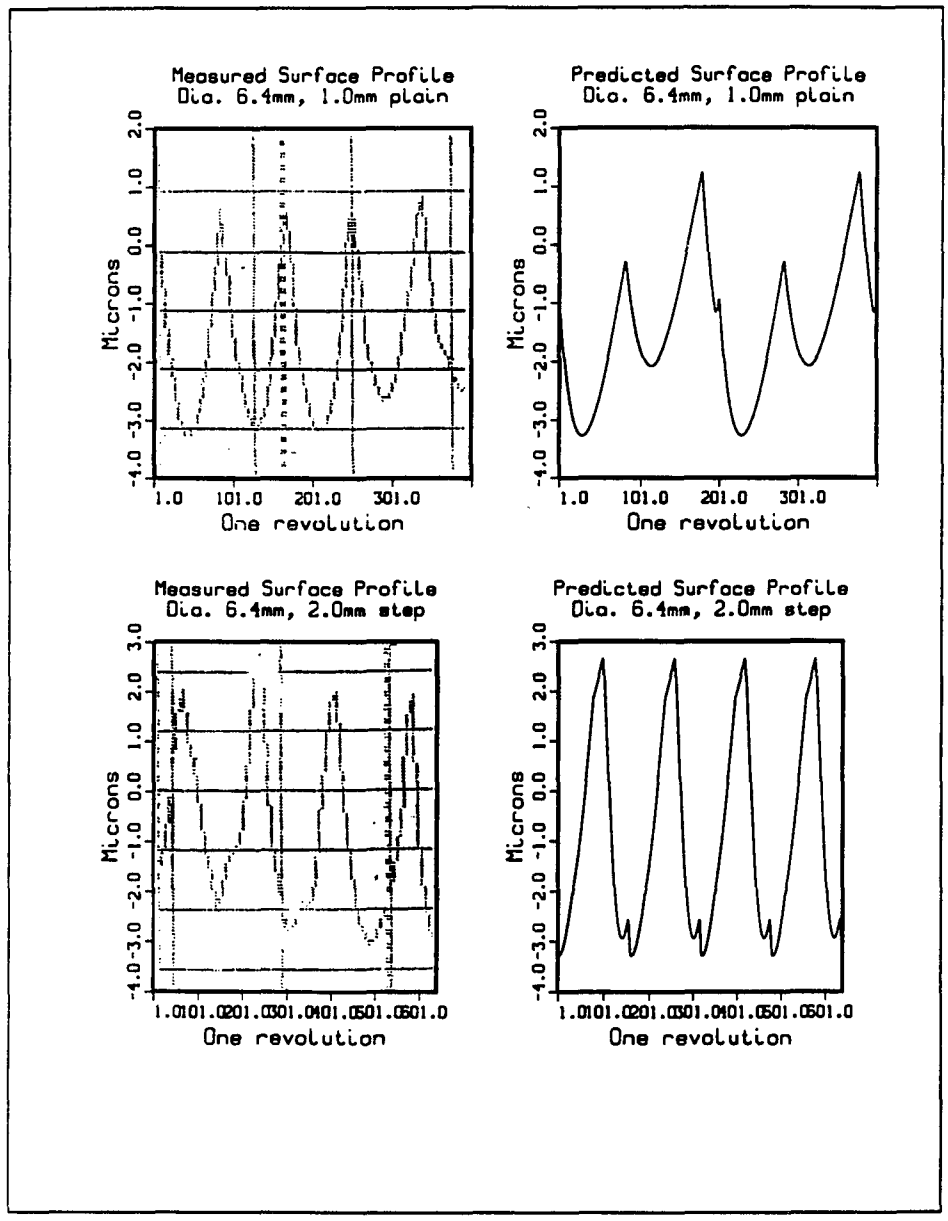

Fig 8.4 Surface profiles, measured and predicted

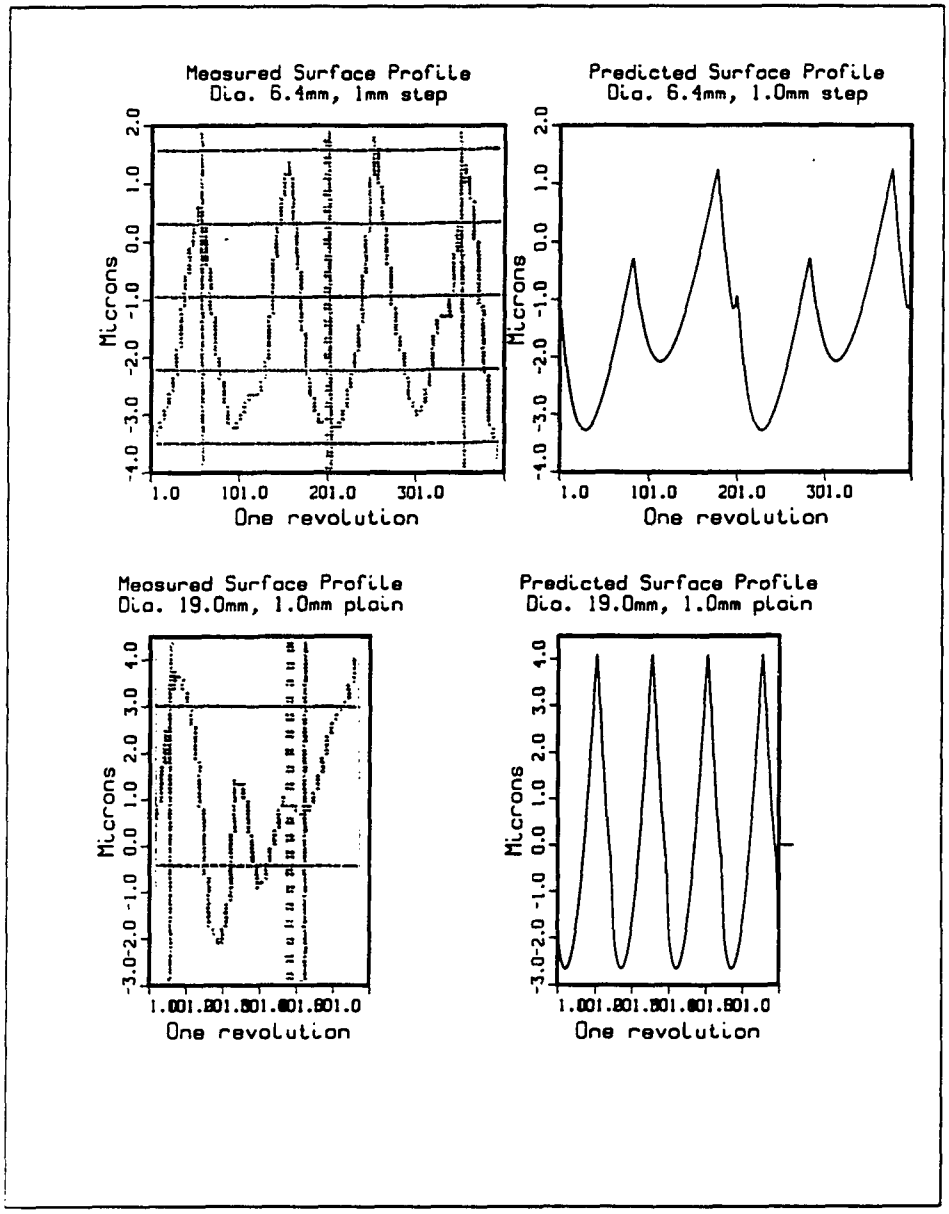

Fig 8.5 Surface profiles, measured and predicted

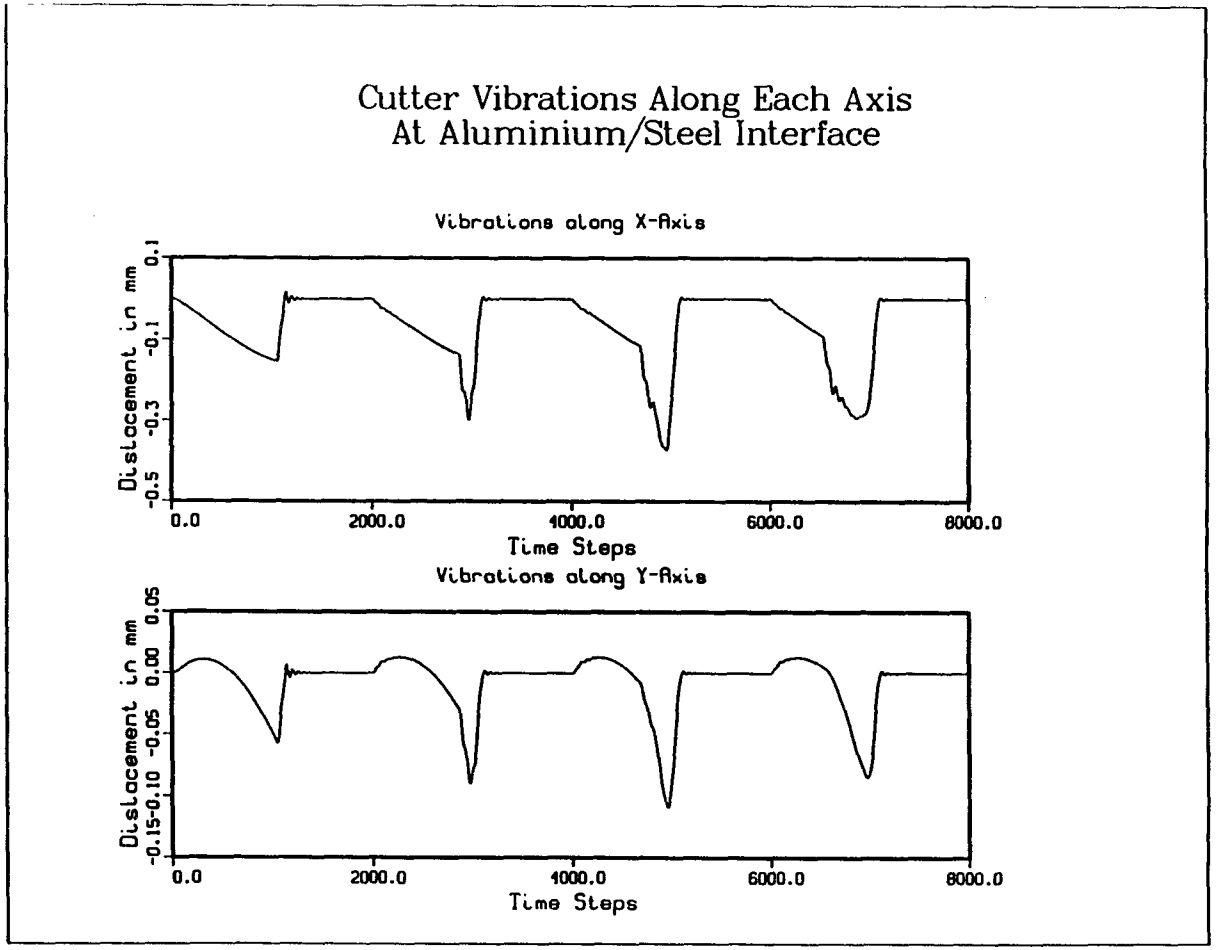

Fig 8.6 Cutter vibrations for composite material

CHAPTER 9

DESIGN SYNTHESIS

The design synthesis for a machining process includes selection of the appropriate tools and process parameters. In case of milling, this consists of the selection of the cutter (e.g. cutter diameter, helix angle, number of teeth) and process parameters (speed, feed, radial and axial depths of cut). An analysis of the dynamic model indicates that all these parameters are intrinsically linked to the surface finish. While some parameters appear to be independently related to the surface finish, certain cross checks are necessary to ensure that the values selected do really represent the optimum set. Selection of each variable is discussed below.

9.1 Selection of computational parameters

A sensitivity analysis of the various input parameters was made and the results are shown in fig 9.1 on page 75. It can be seen that if the number of time steps chosen in one revolution is less than 8000, the dynamic equations of motion fail to converge. For certain situations more time steps may be necessary. But a minimum of 8000 is necessary.

The number of levels dividing the axial depth depend on the axial depth. The thickness of the cutter slice is important. It is seen that for a cutter slice thickness of 0.5 mm, consistent results for the surface finish are obtained.

The number of points selected in one feed per tooth sample length, for surface finish calculations, also affect the surface finish calculation. It is seen that with more than 100 points selected, consistent results are obtained.

The damping ratio for the cutter also affects the surface finish calculations. With a damping ratio of between 0.01 and 0.15 consistent results are obtained. These values are also used by other researchers.

9.2 Selection of the cutter parameters

From the rigid cutter model, it is clear that as the cutter diameter increases, all other variables remaining constant, the surface finish improves. Hence it is appropriate to select the maximum diameter possible for a given situation. The part geometry features are the deciding criteria. For example if a slot is to be milled, the slot width is the limitation. If pockets are to be milled, the maximum allowable corner radius, is the limiting cutter radius. If the pocket has islands, then the minimum space between islands, or between islands and pocket wall, is the limitation. The appropriate cutter diameter can then be selected using a feature extraction program.

However, the selection is subject to the constraint discussed in section 9.3.

From the rigid cutter model, it can be inferred that as the number of teeth increases, the surface finish improves. However, as the number of teeth increase, the flute size decreases, limiting the space necessary for the free flow of chips. Metal removal is hampered, limiting the speed and feed that can be used. The maximum number of teeth that a milling cutter can have is limited. Further the number of teeth is also limited by the constraint described in section 9.3.

As the cutter length increases, its deflection increases, thereby worsening the surface finish and increasing the tolerance. Therefore, it is necessary to select as small a cutter length as possible. The workpiece geometry may dictate the selection of the cutter length in certain situations. For example to reach the bottom of pockets, it may be necessary to have a cutter length of at least the depth of the pocket.

9.3 Selection of process parameters

It is clear from the surface generation mechanism in milling, that only a small portion of cutter tooth path affects the surface finish. Deflection or vibrations in this portion, are detrimental to surface finish and tolerance. An analysis of the dynamic model shows that the cutter deflects when any tooth is cutting the workpiece, starts vibrating when it loses contact with the workpiece, and follows the trochoidal path after the vibrations die down. The zones for a four teeth cutter are shown in fig 9.2. Similarly the region of interest which determines the surface finish, will depend on the surface finish required and the number of teeth. These regions for every teeth are also shown in fig 9.2 below.

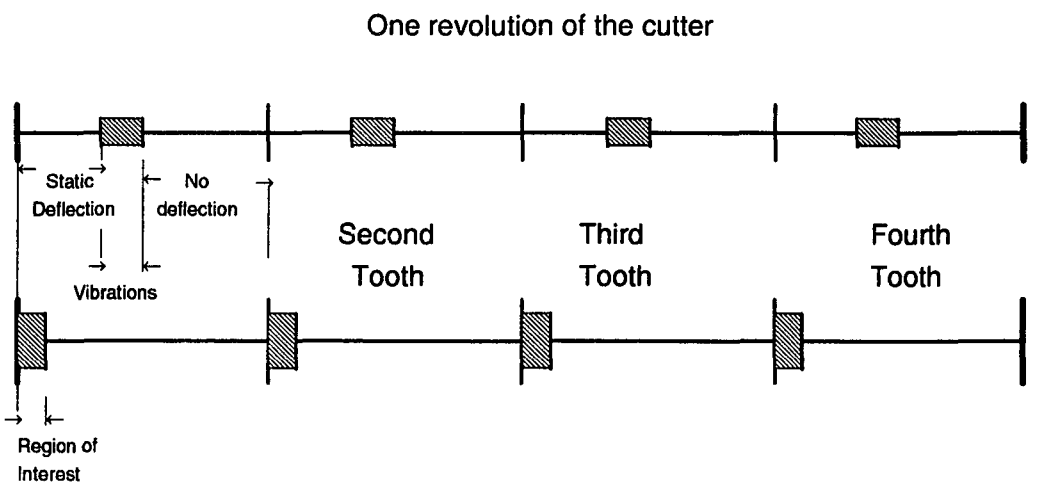

Fig 9.2 Various regions in one cutter revolution

The point where the tooth leaves all contact with the workpiece is determined by the cutter diameter, radial and axial depth of cut and the helix angle. The point where the tooth at the bottom most level leaves the workpiece is given by $\cos^{-1}\ \cos^{-1}\frac{Dc-2d_r}{D_c}$ and the top most level trails this tooth by $2d_a\frac{\tan\alpha}{D_c}$, where d_a and d_r are axial and radial depths of cut respectively. Hence the cutter angle at which the vibrations start are given by

$$\theta_{VS} = \cos^{-1} \frac{D_c - 2d_r}{D_c} + 2d_a \frac{\tan\alpha}{D_c}$$

If the vibrations last for an angle of θ_V then the vibration region ends at

$$\theta_{Ve} = \theta_{VS} + \theta_V$$

These will be periodic and have a period of $\frac{2\pi}{n}$.

The region of interest depends on the surface finish desired and is given by $\cos^{-1} \frac{D_c - 2h}{D_c}$, where h is the desired surface finish. This region is also periodic with a period of $\frac{2\pi}{n}$. The start and end points of these regions are given by

$$\theta_{is} = \frac{2\pi}{n}(i-1) \quad i = 1,2,3, ...$$

$$\theta_{ie} = \theta_{is} + \cos^{-1} \frac{D_c - 2h}{D_c}$$

If these two regions overlap, then the vibrations will affect the surface finish. The vibrations are strong at the beginning and die down with time. If the overlap is at the beginning of the vibration period, then its effect will be severe and the worst possible surface finish will be obtained. If this overlap is at the end of the vibration region, then the effect will be less.

Assuming that the cutter is selected first, the cutter diameter, helix angle and number of teeth can now be taken as fixed. The location and size of the region of interest is now fixed. The vibration zone location can be varied by varying the radial and axial depths of cut as shown in fig 9.2. Proper combination of these to avoid the overlap with vibration region is necessary. Once this is done, the speed and feed can be iterated from the dynamic model to obtain the desired surface finish at the optimum parameter combination.

Alternatively, if the radial and axial depths of cut are to be kept fixed, the cutter parameters can be so selected that the regions do not overlap.

A simulation run for different radial depths of cut was performed. A 6 teeth, 25.4 mm cutter of length 80 mm was chosen. The axial depth of cut was fixed at 5.0 mm. The region of interest

start angle is therefore 60 degrees. Varying the radial depth of cut had the effect of varying the vibration start angle. A plot of surface finish versus the vibration start angle is shown in fig 9.3 on page 76. It can be seen that as the vibration start angle nears the regions of interest, the surface finish starts getting worst. The results are tabulated below.

Table 9.1

Radial Depth of cut mm	Vibration start angle degrees	Uncut surface height (microns) Top	Bottom
1.0	24.9	5.11	6.44
2.0	34.6	5.07	6.50
3.0	42.2	5.01	6.66
4.0	48.7	5.80	7.36
5.0	54.6	7.32	13.06
6.0	60.1	62.70	74.70
7.0	65.3	20.80	20.80
8.0	70.3	17.60	21.12
9.0	75.0	18.30	22.63
10.0	79.7	28.50	31.50

Concluding, the parameter selection has to be done in proper combination, and not individually. Above analysis can only be a guideline.

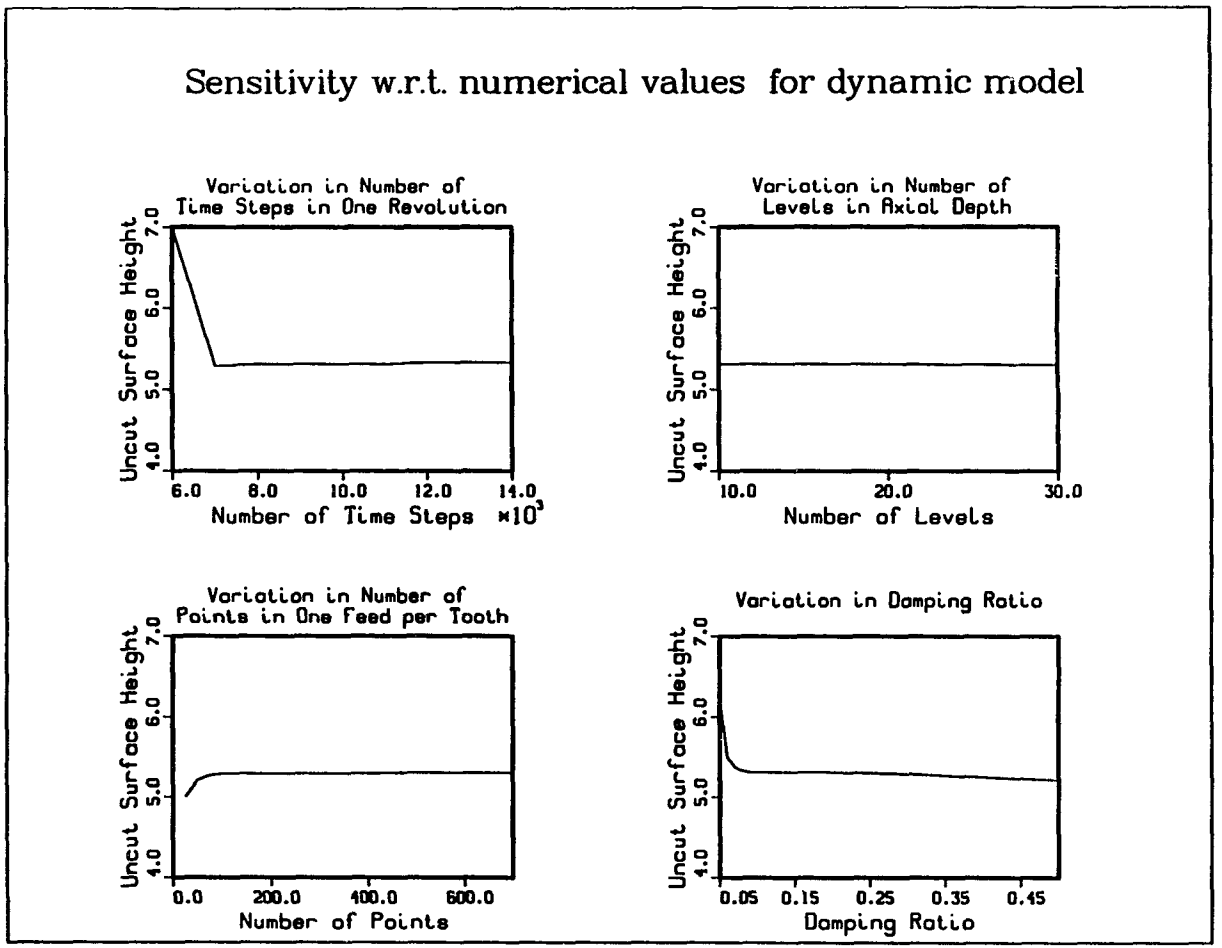

Fig 9.1 Sensitivity w.r.t. numerical values for dynamic model

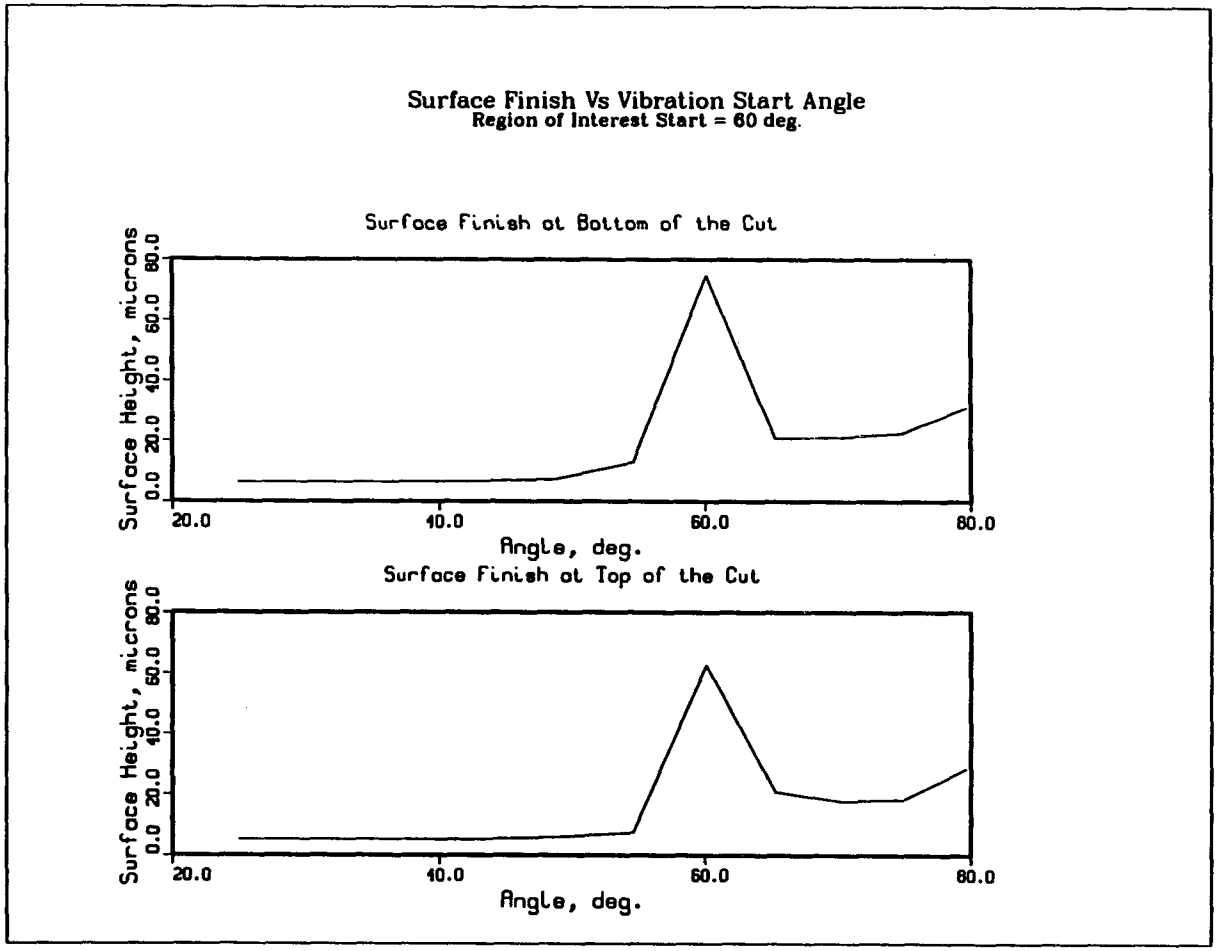

Fig 9.3 Surface finish versus vibration start angle

CHAPTER 10

DISCUSSION AND CONCLUSIONS

A dynamic model for the end milling operation has been developed. Cutter variables, workpiece properties and process variables have been taken into account for modeling the vibrations of the cutter, and computing the surface generated. Surface finish and tolerance is computed from the generated surface. An iterative process is set up to compute the speed and feed required to achieve a desired surface finish. The surface generation process is examined in details, and an insight is obtained to select various cutter and process parameters.

The model incorporates single point orthogonal cutting model to predict the milling forces. The force constant computed has been verified from experiments carried out by Montgomery and Altintas [16], with HSS cutter and Aluminum T 7075 workpiece. It is necessary to carry out further experiments for other combinations of tool and workpiece material. The force variation with cutter rotation also needs to be experimentally verified.

Cutter displacements are computed using a mass spring damper system representation for the cutting system. The dynamic equations used for the cutting action are also capable of predicting chatter. There are three known effects leading to chatter. They are: the regenerative effect, mode coupling and velocity dependence. The regenerative effect has been taken into account, because the chip thickness is computed from the path traveled by the previous tooth. Any waviness in the surface left behind by the previous tooth is already taken into account. As for mode coupling, the two modes of vibration, in the X and Y direction, are assumed to be independent. Model coupling can be built into the model if necessary. The velocity dependent effect for the spring constant has not been taken into account. The spring constant for the cutter is assumed to be constant. This can also be built into the model. However, the computing time at

present, without these enhancements, is quite high. Depending on the depth of cut and features, it takes 15 to 50 minutes of CPU time per iteration, to run the model on Convex, computer. Therefore the cost of incorporating these enhancements versus the increase in accuracy of the predictions, must be considered carefully.

The model is a general purpose one and does not take into account the machine tool variables like machine dynamics, spindle run out and positioning accuracy. These need to be built into the model, to take into account the peculiarities of each machine tool. The dynamic constants of the machine are important, specially in milling features. It was observed that these induced vibrations in the machine slides and headstock, along with vibrations in the cutter. The cutter vibrations may or may not affect the surface finish, depending on where the vibration region is. However, other vibrations will affect the surface finish. It is therefore recommended to modify the dynamic model for plain cuts, to incorporate the machine tool variables, before proceeding on further investigations with features.

The dynamic model, apart from its original purpose of predicting speed and feed for a desired surface finish, will serve as a tool to investigate the milling operation as a surface generating process in metal cutting. A variety of situations could be simulated with modifications to the base model.

Long computing time is a limitation to the use of this model on line. However as faster computing machines become available in the future, the possibility of its use in on line simulation cannot be ruled out. Till then this model will have to be used as an off line analytical tool.

APPENDIX A

DESCRIPTION OF MODULES

Main:

Contains the main program. The iteration process is also in this program.

Input:

Reads the input from the input file. Variables required for the program, like shear plane angle, shear plane stress are computed from the material properties. Degrees are converted to radians.

Output:

Outputs the input quantities as well as the program output, like required speed, feed, results of successive iterations, surface finish and tolerance at the bottom and top of the cut.

Rgdmdl:

Computes the feed required to achieve the necessary surface finish based on the rigid model, with maximum speed as the constraint.

Rgfmdl:

Computes the speed required to achieve the necessary surface finish based on the rigid model, with maximum feed as the constraint.

Defmdl:

Computes the surface finish and tolerance at the top and bottom of the cut, given the speed and the feed. Calls the following subroutines:

Actpos:

Computes the actual position of all teeth, at all levels and at all time steps and stores them as x - y coordinates in two 3 D arrays. Calls the following subroutines:

Deflection:

Computes the deflection at all points along the cutter axis in the x and y directions, at any given time step. These are stored as a two 2D arrays. Calls the following subroutines:

Force:

Computes the force at any given time, for any given level.

Def:

Computes the deflection at any point along the cutter axis due to the above force, modeling the cutter as a cantilever beam.

Uncut:

Computes the uncut surface height for any point along the feed axis, at any level.

Dynmdl:

Computes the surface finish and tolerance at the top and the bottom of the cut, for a given speed and feed. Calls the following subroutines:

Actdpos:

Computes the actual position of all teeth, at all levels and at all time steps and stores them as x - y coordinates in two 3 D arrays. Calls the following subroutines:

Eqforce:

Computes the equivalent force acting at the center of the axial depth of cut, that is used for dynamic analysis. Calls the following subroutine:

Chipthkf:

Computes the chip thickness for any tooth, at any level, at any time step. Depending upon the tooth position, chip thickness is computed with respect to the geometric feature and the previous tooth path, or with

respect to the final depth of cut. Chip thickness with respect to the previous tooth is computed by linear interpolation between the present tooth position and the path followed by the previous tooth.

Chipthks:

Computes the chip thickness with respect to the geometric feature. This is done by representing the feature by a parametric cubic curve and computing its intersection with the present tooth position.

Jacob:

Computes the Jacobian for the interpolation required for computing the intersection.

Solve:

Solves the Jacobian for the above.

Filter:

Filters out vibrations with frequency more than 120% of the natural frequency.

Disc:

Computes displacements along the cutter axis, given the dynamic displacement at the center of the axial depth of cut.

Uncut:

Uses the same subroutine as above, to compute the uncut surface height at any point along the feed axis at any level.

APPENDIX B

LIST OF VARIABLES

d_a	axial depth of cut
d_r	radial depth of cut
D_c	cutter diameter
f_t	feed per tooth
F	feed
F_t	tangential cutting force
F_n	normal cutting force
k_n	force constant in normal direction
k_t	force constant in tangential direction
L	cutter length
m	mass of the cutter
n	cutter rpm
N_l	number of levels
P_{sp}	specific power
T	number of teeth
T_n	number of time steps
α	helix angle of the cutter
β	shear angle
γ	rake angle of the cutter
η	friction angle

REFERENCES

[1] Smith, S., and Tlusty, J., "Modelling and Simulation of the Milling Process," Trans. of ASME, Vol. 113, May 1991.

[2] Wang, W. P.,"Solid Modeling for Optimizing Metal Removal of Three Dimensional End Milling," Journal of Manufacturing Systems, Vol. 1, 1988, pp 57-66.

[3] DeVor, R. E., and Kline, W.A., "A Mechanistic Model for the Force System in End Milling ," Proc. of NAMRC 8, May 1980, SME.

[4] Tlusty, J. and MacNeil, P. "Dynamics of Cutting Forces in End Milling," Annals of the CIRP, Vol. 24, 1975.

[5] Tlusty, J., "Machine Dynamics," Handbook of High Speed Machining Technology, R. I. King, ed., Chapman and Hall, New York, 1985.

[6] Hann, V., "Kinetik des Schaftrasens," Ph.D. Dissertation, Technischen Hochschule, Aachen, 1983.

[7] Kline, W. A., DeVor, R. E., and Shareef, I. A., "The Prediction of Surface Accuracy In End Milling," Trans. ASME, Journal of Engineering for Industry, Vol. 104, August 1982, pp 272-278.

[8] Tlusty, J., Cowley, A., Elbestawi, M. A., "A Study of an Adaptive Control System for Milling with Force Constraint," Proc. NAMRC 6, April 1978, SME.

[9] Tlusty, J., Hernandez, I., Smith, S., and Zamudio,, C., "High Speed High Power Spindles with Roller Bearings," Annals of the CIRP, Vol. 36/1, 1987.

[10] Smith, S., and Tlusty, J., "Update on High Speed Milling Dynamics," Symposium on Intelligent Integrated Manufacturing Analysis and Synthesis, PED Vol. 25, ASME 1987 WAM.

[11] Sutherland, J. W., "Dynamic Model of the Cutting Force System in the End Milling Process," Sensors and Controls for Manufacturing, PED Vol. 33, ASME 1988.

[12] Watanabe, T., "Model Based Approach to Adaptive Control Optimization in Milling," Journal of Dynamic Systems Measurement and Control, Trans. ASME, Vol. 108, n1, 1986.

[13] Stephenson, D. A., "Material Characterization for Metal Cutting Force Modeling," Journal of Engineering Material and Technology, Trans. ASME Vol. 111, n2, 1989.

[14] Martellotti, M. E.,"An Analysis of the Milling Process," Trans. of ASME, Vol. 63, pp 667-700, 1941.

[15] Wright, P.K.,"Predicting the Shear Plane Angle in Machining From Workmaterial Strain-Hardening Characteristics," Journal of Engineering for Industry, Vol.104, pp 285-292, 1982.

[16] Montgomery, D., and Altintas, Y., "Mechanism of Cutting Forces and Surface Generation in Dynamic Milling," Trans. of ASME, Vol. 113, pp 160-168, 1991.

[17] Tlusty, J., and Ismail, F., "Special Aspects of Chatter in Milling," Trans. of ASME, Vol. 105, pp 24-32, 1983.